Chemical Engineering Research and Design

Energy Saving Design and Control of Side-Streams Reactive Distillation Configuration for Diphenyl Carbonate Production Process --Manuscript Draft--

Manuscript Number:	CHERD-D-23-02481					
Article Type:	VSI: Sust Dist					
Section/Category:	Process Systems Engineering					
Keywords:	Diphenyl carbonate; Reactive distillation; Side-stream configuration; Thermally coupled configuration; Process Control					
Corresponding Author:	Hao-Yeh Lee, Ph.D National Taiwan University of Science and Technology Taipei, Taiwan TAIWAN					
First Author:	Bangkit Gotama					
Order of Authors:	Bangkit Gotama					
	Tua Halomoan					
	Yu-Ying Chen					
	Hao-Yeh Lee					
Abstract:	Polycarbonate production, a popular material, is a significant concern due to environmental and safety concerns. Alternative methods, like diphenyl carbonate (DPC), have been proposed for production without phosgene. Thermal enhancement techniques on reactive distillation (RD), such as thermally coupled (TCRD) and hybrid heat-integrated (HIRD), have improved energy efficiency and reduced operational and capital costs. Implementing the dual intensification strategy in DPC production, which combines RD with a side-stream configuration, also offers a viable approach to achieving the objectives above and still needs more knowledge. This work proposes a combination of TCRD and HIRD with one side-stream (SS1-TCRD and SS1-HIRD) and two side-streams (SS2-TCRD and SS2-HIRD). The sequential iterative method optimized the design, minimizing total annual cost (TAC). The SS2-HIRD has shown optimal results, saving 47.27% energy usage and 31.46% TAC savings. Moreover, the control structure was applied to SS2-HIRD to maintain product quality and process safety. Among the four proposed control structures, CS4 is an excellent control structure for maintaining feed and composition throughput disturbances with an indication of the smallest IAE value.					
Suggested Reviewers:	Jesus Rafael Alcantara-Avila, PhD jralcantara.consulting@gmail.com He is an expert of this feild.					
	Moonyong Lee Yeungnam University mynlee@ynu.ac.kr					
	San-Jang Wang, PhD National Tsing Hua University wangsj@mx.nthu.edu.tw					
	Renanto Handogo Sepuluh Nopember Institute of Technology renanto@chem-eng.its.ac.id					
	Juan Gabriel Segovia-Hernández, PhD Professor, University of Guanajuato gsegovia@ugto.mx					
	Xin Gao, PhD Professor, Tianjin University gaoxin@tju.edu.cn					

Cover Letter

Cover Letter

October 30, 2023

Dear Editor in Chief of Chemical Engineering Research and Design,

We would like to submit the attached manuscript, "Energy Saving Design and Control of Side-Streams Reactive Distillation Configuration for Diphenyl Carbonate Production Process," for consideration of publication as an original research article in Chemical Engineering Research and Design in the Special Issue on "Challenges and Opportunities in Advanced Processes based on Distillation for Sustainable Processes."

The manuscript addresses a design and control of dual intensification technique integrates side-streams and energy integrated configuration for DPC process. This novel approach could be a benchmark for future advancements in DPC synthesis, as current methods are limited to reactive distillation methods and combination with thermal intensification strategies such as thermally coupled and hybrid heat-integrated configurations. As a result, using this dual intensification strategy can lower energy usage and increase TAC savings on DPC production process. The best configuration among them is two side-streams with hybrid heat-integrated reactive distillation (SS2-HIRD). Among the four proposed control structures, CS4 of SS2-HIRD is an excellent control structure for maintaining feed and composition throughput disturbances with an indication of the smallest IAE value.

We confirm that this article has not been submitted to any other journal.

Sincerely yours,

Hao-Yeh Lee (Professor)

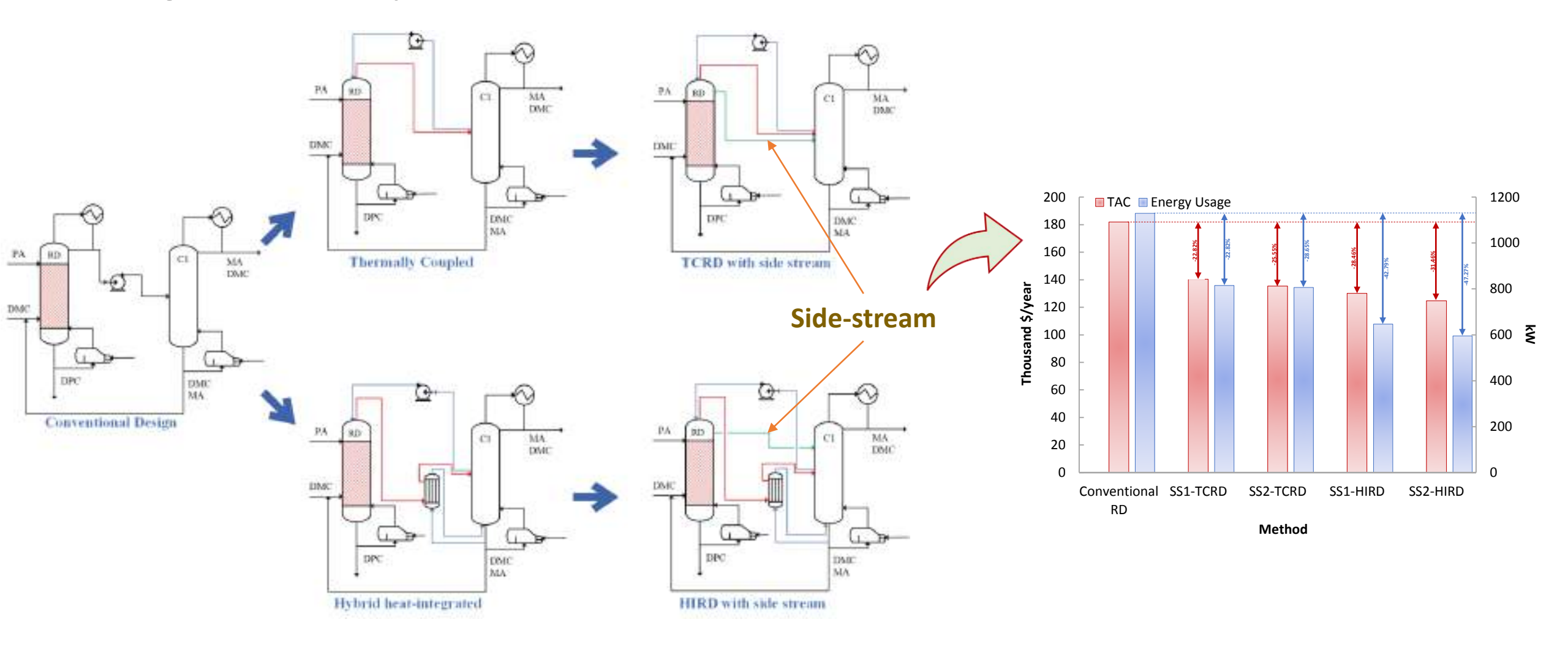
Department of Chemical Engineering,

National Taiwan University of Science and Technology

Taipei 10607, Taiwan

E-mail: haoyehlee@mail.ntust.edu.tw

Integration side-stream with intensified RD configurations in DPC production



Highlights

- Side-stream configurations combined with TCRD and HIRD are proposed for DPC production.
- SS2-HIRD provides the lowest energy consumption and the highest TAC savings compared to conventional RD.
- A robust control strategy with a lower IAE value, CS4 of SS2-HIRD, is proposed to obtain the desired product purity.

Energy Saving Design and Control of Side-Streams Reactive Distillation Configuration for Diphenyl Carbonate Production Process

Bangkit Gotama^{a,b†}, Tua Halomoan^{a†}, Yu-Ying Chen^a, Hao-Yeh Lee^{a,*}

Hao-Yeh Lee, Email: haoyehlee@mail.ntust.edu.tw

^a Department of Chemical Engineering, National Taiwan University of Science and Technology, Taipei 10607, Taiwan

^b Department of Chemical Engineering, Institut Teknologi Kalimantan, Jl. Soekarno-Hatta KM 15, Balikpapan, 76127, Indonesia

[†] These authors contributed equally to this work

^{*}Correspondence concerning this article should be addressed to:

Abstract

Polycarbonate production, a popular material, is a significant concern due to environmental and safety concerns. Alternative methods, like diphenyl carbonate (DPC), have been proposed for production without phosgene. Thermal enhancement techniques on reactive distillation (RD), such as thermally coupled (TCRD) and hybrid heat-integrated (HIRD), have improved energy efficiency and reduced operational and capital costs. Implementing the dual intensification strategy in DPC production, which combines RD with a side-stream configuration, also offers a viable approach to achieving the objectives above and still needs more knowledge. This work proposes a combination of TCRD and HIRD with one side-stream (SS1-TCRD and SS1-HIRD) and two side-streams (SS2-TCRD and SS2-HIRD). The sequential iterative method optimized the design, minimizing total annual cost (TAC). The SS2-HIRD has shown optimal results, saving 47.27% energy usage and 31.46% TAC savings. Moreover, the control structure was applied to SS2-HIRD to maintain product quality and process safety. Among the four proposed control structures, CS4 is an excellent control structure for maintaining feed and composition throughput disturbances with an indication of the smallest IAE value.

Keywords: Diphenyl carbonate, Reactive distillation, Side-stream configuration, Thermally coupled configuration, Process Control.

1. Introduction

Polycarbonates (PCs) are a class of engineering thermoplastics with notable mechanical, optical, electrical, and heat-resistant characteristics [1], [2]. Over the past few decades, the predominant commercial approach for synthesizing polycarbonate (PC) has primarily involved the interfacial polycondensation of bisphenol A (BPA) with phosgene [3]. Regrettably, the procedure is associated with environmental and safety concerns due to the poisonous compound phosgene and the substantial consumption of methylene chloride and water [1], [3]. To address the challenges mentioned above, it is imperative to employ alternative methods that are both safer and more environmentally friendly to supplant phosgene as a precursor [4].

Several studies have proposed alternative methods for manufacturing PCs that do not rely on phosgene. These processes utilize diphenyl carbonate (DPC) as a precursor, involving a two-step transesterification process. Subsequently, the resulting methyl phenyl carbonate (MPC) undergoes disproportionation to yield DPC and dimethyl carbonate (DMC). Various works have discussed these alternative methods [5], [6]. In addition, these methods provide several advantages due to their absence of azeotropes, side reactions, and high equilibrium constants [7], [8].

Presently, there is a global endeavor to diminish the reliance on fossil energy sources, which is being pursued by implementing diverse policies. These policies encompass the adoption of environmentally friendly and sustainable energy sources, the enhancement of energy efficiency, and the complete abandonment of fossil fuels. Energy efficiency is of paramount importance in the realm of process intensification (PI) within the chemical industry [9]. It can significantly enhance process safety, economic viability,

and production yield and reduce waste generation, emissions, and raw material usage through novel process and equipment designs [10], [11]. As an application of PI, reactive distillation (RD) is a process integration technique that integrates reactions with distillation within a single process unit. This alternative structure can enhance conversion rates while decreasing energy requirements, operational costs, and capital expenditures compared to the conventional system with a reactor followed by distillation. Additionally, RD can mitigate chemical equilibrium limitations and thermodynamic constraints [12]–[15].

The current feasibility of investigating the RD system's thermal enhancement, aiming to improve the economic viability of distillation operations, remains despite the escalating operational expenses and the environmental apprehensions regarding greenhouse gas emissions [11]. Various publications have proposed diverse configurations of intensified RD for the synthesis of DPC, including thermally coupled design [7], heat-integrated stages [16], thermally coupled with heat-integrated stages [17], double-effect heat integration [18], hybrid heat-integrated [18], and heat integration through vapor recompression system [19]–[21]. The hybrid heat-integrated RD configuration (HIRD) is proposed as a promising alternative that combines the advantages of both thermally coupled RD (TCRD) and double-effect heat integration (DERD). A pressurized approach without a compressor, similar to DE, can potentially increase energy efficiency by 34% [18].

Implementing the dual intensification strategy, as proposed by Kong et al. [11], which involves the integration of RD with a side-stream configuration, presents an alternative approach towards achieving enhanced energy conservation, reduced impact on the environment, and increased profitability within the context of sustainable production.

However, to date, there is a need for more scholarly research that elucidates this phenomenon, particularly in the context of implementation within the RD configuration [22], [23]. Side-stream structures are commonly employed in conjunction with reactive-extractive distillation [24], [25], extractive distillation [26]–[29], and conventional distillation sequences [30], [31]. Luyben [32] suggests that liquid side-stream columns are frequently used in ternary systems where the smallest and lightest components are involved. The intermediate component is separated from a liquid side-stream and collected as a liquid from a tray above the feed tray. Therefore, the current configuration requires a substantial difference in volatility between the least heavy and middle components. This particular demand can be easily met within the framework of DPC synthesis.

This study aims to provide an advanced design for a side-stream RD configuration to enhance energy efficiency and cost-effectiveness in the manufacturing of DPC compared to conventional designs. We formulated and optimized four scenarios to minimize the total annual cost (TAC). These scenarios include using one side-stream in TCRD (SS1-TCRD) and two side-streams in TCRD (SS2-TCRD). Additionally, we explored the use of one side-stream in HIRD (SS1-HIRD) and the utilization of two side-streams in HIRD (SS2-HIRD). Furthermore, our work aims to evaluate the most efficient performance of the steady-state design procedure for assessing control systems that ensure product quality and process safety.

2. Kinetic and thermodynamic model

2.1 Kinetic model

The synthesis of DPC from DMC and PA (Phenyl Acetate) is a two-step reversible reaction. Equations (1) and (2) illustrate the transesterification reactions involving DMC and PA, leading to the formation of MPC and MA (Methyl Acetate). In contrast, the transesterification reaction between MPC and PA yields DPC and MA. Additionally, equation (3) represents the disproportionation of MPC into DPC and DMC [7].

$$DMC + PA \leftrightarrow MPC + MA \tag{1}$$

$$MPC + PA \leftrightarrow DPC + MA$$
 (2)

$$2MPC \leftrightarrow DPC + DMC$$
 (3)

The rate expressions for these reversible reactions are given by equations (4) through (6):

$$r_1 = k_{f_1}[DMC][PA] - k_{b_1}[MPC][MA]$$
 (4)

$$r_2 = k_{f_2}[MPC][PA] - k_{b_2}[DPC][MA]$$
 (5)

$$r_3 = k_{f_3}[MPC]^2 - k_{b_3}[DPC][DMC]$$
 (6)

Here, r_i represents the reaction rate of the *i*-th reaction in kmol/m³s, while k_{f_i} and k_{b_i} denote the forward and backward reaction rate coefficients, respectively. The molar concentration of each component, denoted as $[C_j]$, is expressed in kmol/m³. The Arrhenius equation represents the equilibrium rate constant of the reaction. For detailed kinetic parameters, such as the pre-exponential factor (k_0) and the activation energy (E_a) , please refer to Table S1, which was compiled from kinetic regression results conducted by Cheng et al. [7].

2.2 Thermodynamic model

In a phosgene-free reaction system for Diphenyl Carbonate (DPC) production, all components exhibit a significant range of normal boiling points, arranged in the following order: MA (57.1 °C) < DMC (90.2 °C) < PA (195.7 °C) < MPC (234.7 °C) < DPC (302 °C) [17]. Furthermore, the absence of an azeotrope in every binary vapor-liquid equilibrium has been verified by Yao [33] and simulated using Aspen Plus V.11, as depicted in Figure S1 (Supplementary Data). Consequently, the simulation environment employs an ideal model to elucidate the thermodynamic correlation among all constituents. The vapor pressure of each component was determined using the Antoine equation in the simulation. The parameters utilized in this investigation were obtained from Lee et al. [18], as documented in Table S2 of the Supplementary Data.

3. Process optimization

Total annual cost (TAC) evaluation was used to determine the optimized design of DPC production. The TAC evaluation of the optimized design focuses on assessing its total operating cost (OC) and annualized capital cost (CC) within a specified payback time (three years). The OC consists of steam, cooling water, and catalyst. Meanwhile, the CC includes the costs of the column shell and trays, condenser, and reboiler. The Aspen Plus Economic Analyzer (APEA) tool in Aspen Plus V.11 was utilized to calculate the TAC of configurations. Equation (7) illustrates the calculation of the TAC.

$$TAC = OC + \frac{CC}{Payback\ Period} \tag{7}$$

Although the method was time-consuming, the ideal design of the flowsheet was accomplished by employing sequential iterative optimization techniques. Despite the potential applicability of global optimization techniques, such as the simulated annealing algorithm (SAA) [34], their practical implementation could be improved. Hence, the manual segmentation of recycling streams was vital in ensuring precise outcomes.

The optimization procedures in all designs were applied to optimize six variables: <1> total number of stages in the RD column (NT_{RD}), <2> location of feed PA (NF_{PA}), <3> location of feed DMC (NF_{DMC}), <4> location of feed recycling (NFR_{CY}), <5> location of feed steam head (NF_{DST}), and <6> total number of C1 stages in the column (NT_{C1}). In particular side-stream configurations, apply additional variables including <7> location of first side-stream (NF_{SS-1}), <8> flow rate of first side-stream (F_{SS-1}), <9> location of first feed side-stream in C1 column (NF_{SS-IN-1}), <10> location of second side-stream (NF_{SS-2}), <11> flow rate of second side-stream (F_{SS-2}), and location of second feed side-stream in C1 column (NF_{SS-IN-2}). In addition, the operational variables encompass the adjustment of the reboiler duty in the RD column, denoted as QR_{RD}, to meet the product specification of DPC. Similarly, the adjustment of the RR in column C1 (RR_{C1}) is performed to meet the specification of the by-product MA. Lastly, the reboiler duty in column C1 (QR_{C1}) is adjusted to satisfy the purity specification of the unreacted DMC.

4. Side-stream configuration on RD of DPC production

The research employs indirect conventional RD as the base case design. When replicating the design, we consult reference [7] for details about the flow rate, feed composition, and product. Nevertheless, considering the temperature at which the catalyst

decomposes, the column configuration was modified and refined, as previously documented in the publications authored by our research group [17], [18]. Based on the findings of the optimization analysis, the total energy requirement in the specified design is determined to be 1129,643 kW. The optimal TAC is computed to be $$181.9 \times 10^3$ per year.

The primary objective of examining this particular arrangement is to analyze the occurrence of the remixing effect phenomenon in both the upper and lower columns. The DMC remixing yields outcomes whereby the proportion of the MA component is progressively augmented towards the uppermost section of the RD column. Conversely, in the lower segment, the remixing of PA is achieved through the combination of the DMC recycling liquid stream and the RD column internal vapor stream [17].

The phenomena of remixing effect can be effectively addressed using a thermally coupled design, as explored in our prior research [17]. This approach has been acknowledged as a viable alternative that mitigates the remixing effect and enhances energy efficiency by a significant margin of up to 24.5%. Moreover, implementing heat integration in the HIRD process might result in a nearly twofold reduction in energy consumption compared to the conventional RD [18] when the working pressure at the RD and C1 columns is modified. However, it is essential to note that this modification also eliminates the remixing effect. The design concept is realized by integrating advantages derived from thermally coupled and double-effect configurations.

Our preliminary analysis determined that integrating conventional RD with sidestream arrangements did not eliminate the remixing impact despite its potential to minimize energy usage. Hence, integrating side stream design with either TCRD or HIRD can yield the optimal design for DPC production, as elaborated in the subsequent section.

4.1 TCRD with side-stream (SS-TCRD)

Establishing the column specifications for RD in SS-TCRD differs significantly from traditional RD, mainly due to side-stream inclusion. The best location of the PA feed stage establishes the optimization results and determines the number of stages in the rectifying and reaction zones. The last stage, which pertains to the stripping zone, is established by considering the temperature threshold for catalyst deactivation. The separation efficiency of the column typically exhibits an upward trend with an increase in the total number of stages, RD, and C1 columns, resulting in a reduction in energy consumption. Nevertheless, this will also increase the TAC.

In the context of the sequential iterative optimization technique, it is imperative to adjust the design variables to ascertain their sensitivity, specifically regarding their influence on changes in the TAC as the objective function. The initial variable optimized in the iterative optimization technique will have the highest sensitivity. In SS1-TCRD, the optimization method used nine variables: NT_{RD}, NF_{PA}, NF_{DMC}, NFR_{CY}, NF_{DST}, NT_{C1}, NF_{SS-1}, F_{SS-1}, and NF_{SS-IN-1}. In the SS2-TCRD, it is essential to consider additional design factors arising from a second side-stream, including NF_{SS-2}, F_{SS-2}, and NF_{SS-IN-2}. In the present arrangement, the pressure exerted on columns RD and C1 remains constant at 1.06 atm and 1 atm, respectively.

Based on the findings of sensitivity analysis in SS1-TCRD, it has been determined that F_{SS} and NF_{SS} are design variables that substantially impact changes in the TAC. This

phenomenon arises because of the significant influence of the F_{SS} on the RD column's energy demand. Consequently, if the F_{SS} increases, the energy needed for the column will drop, impacting the energy usage for the reboiler duty on the RD column. In the context of the SS2-TCRD, it is worth noting that while the sensitive variables, namely F_{SS} and NF_{SS}, hold significance, they are not prioritized as the initial variables for optimization. The initial design factors to be optimized encompass NF_{PA} and NF_{DMC}. In order to accommodate the placement optimization of the side streams inside the rectifying section, it is necessary to have an adequate number of stages, as two side streams will be introduced into the process. Consequently, the optimization of NF_{PA} and NF_{DMC} will be prioritized. Furthermore, F_{SS} and NF_{SS} are sensitive design variables that need further optimization.

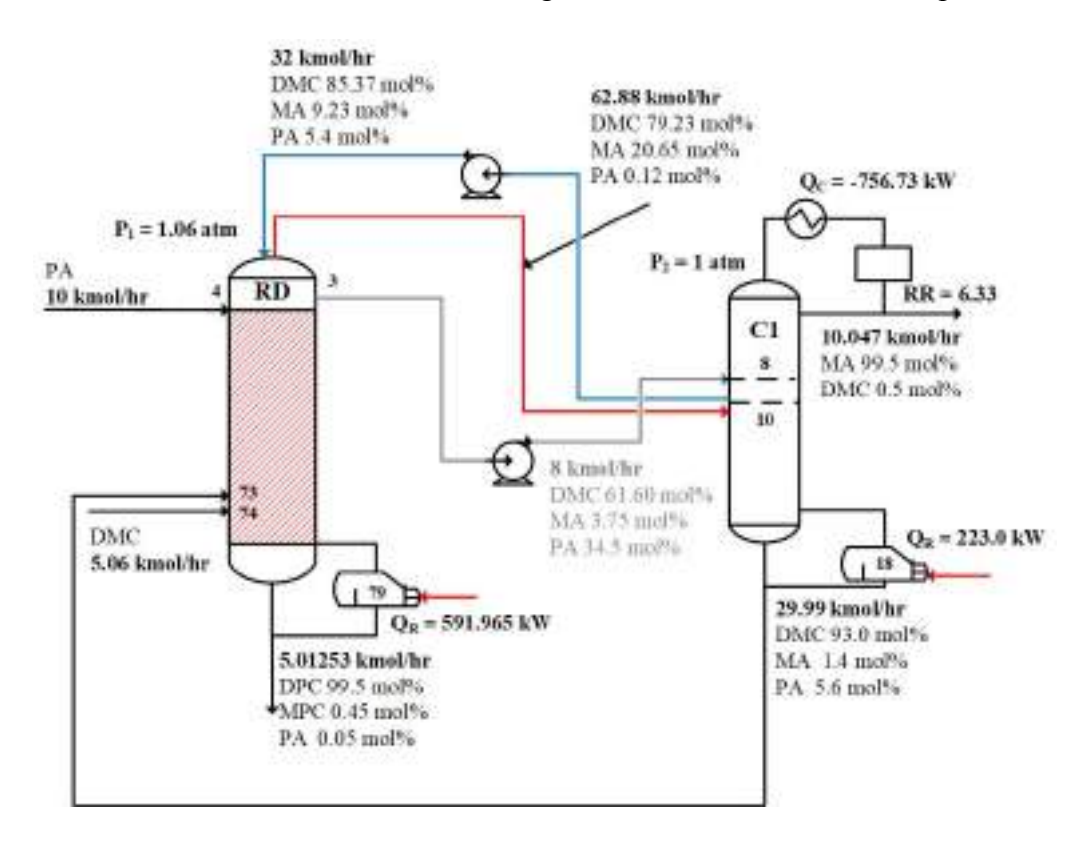


Figure 1. Result of optimum flowsheet for SS1-TCRD.

The NF_{SS} can be situated within this arrangement in three distinct zones: rectifying, reaction, and stripping. The rectifying zone is considered the most suitable NF_{SS}. The prevalence of light components, particularly DMC and MA, is more pronounced in the composition than heavy components. Utilizing F_{SS} to reintroduce intermediate or light components into the subsequent separation column is generally better. The suboptimal quality of the side-stream in the reaction zone can be attributed to its composition, which predominantly comprises heavy components. These components significantly impact the temperature, hence establishing favorable conditions for the conversion process. Due to the prevalent utilization of DPC products in the lower portion of the stripping section, including a side-stream at the base of the column is rendered unnecessary.

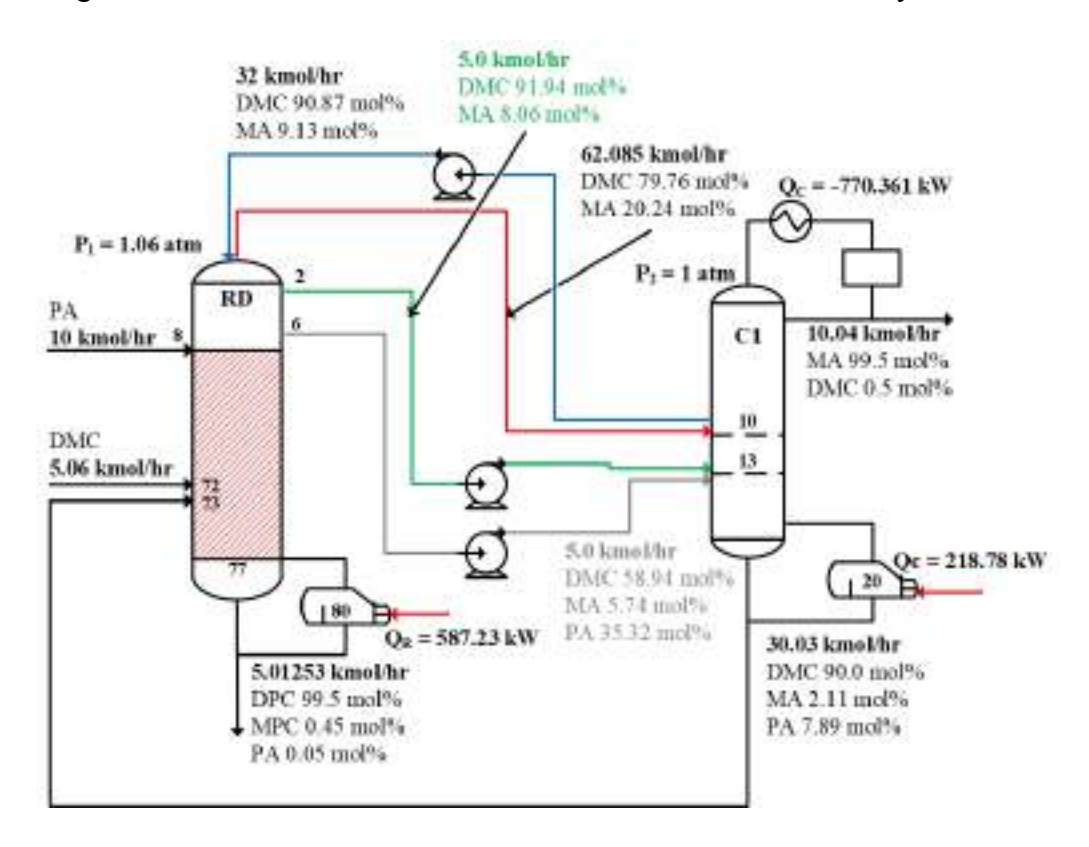


Figure 2. Result of optimum flowsheet for SS2-TCRD.

Consequently, the side-stream configuration in both SS1-TCRD and SS2-TCRD exhibits a notable reduction in energy consumption and a corresponding rise in TAC reductions, as illustrated in Table 1. The utilization of SS1-TCRD and SS2-TCRD has demonstrated the ability to effectively diminish reboiler duty by a maximum of 27.88% and 28.64%, correspondingly, while also reducing TAC by up to 22.82% and 25.55%, respectively, in comparison to conventional RD. The optimization findings indicate that the introduction of F_{SS} to the C1 column (specifically, eight kmol/h on SS1-TCRD and a total of 10 kmol/h on SS2-TCRD) resulted in a reduction of unconverted DMC to 90-93 mol%. This reduction in unconverted DMC contributed to achieving a higher purity of 99.5 mol% for DPC and MA products, as illustrated in Figures 1 and 2. Insufficient purity of the DMC recycling stream can impact the RD column's temperature drop. This factor may influence the conversions of products in the RD column.

Table 1. Summary result of the optimal design of side-stream with TCRD and HIRD.

		Reboil	er Duty	Total	Condenser	
Configuration	TAC	(k)	W)	Reboiler	C1 Duty	
	$(10^3 \text{\$/year})$	RD	C1	Duty	(kW)	
				(kW)		
Conventional	181.9	785.22	344.423	1129.643	-332.63	
SS1-TCRD	140.39	591.965	223.0	814.965	-756.73	
SS2-TCRD	135.42	587.23	218.78	806.01	-770.361	
SS1-HIRD	130.13	646.23		646.23	-632.350	
SS2-HIRD	124.67	595.6		595.6	-581.29	

4.2 HIRD with side-stream (SS-HIRD)

Advantages can be observed when the side-stream is implemented inside a TCRD (SS-TCRD). In addition to mitigating the energy consumption associated with the reboiler duty in columns RD and C1, side-streams can yield cost savings in operational activities. Nevertheless, the suitability of the side-stream layout inside the TCRD is restricted in instances where F_{SS} increases, and there is a corresponding increase in the amount of energy consumed at column C1. To retain the purity of DPC, it is necessary to employ a duty reboiler within column C1, which serves the purpose of heating the low-quality unreacted DMC. Consequently, the implementation of an HIRD is used as a means to address this constraint. The reboiler duty in column C1 is removed and substituted with a heat exchanger to transfer latent heat from the top of the RD column to the bottom of column C1.

The sequential iterative optimization methodology employed in SS-HIRD is analogous to that of SS-TCRD, with the utilization of nine variables in SS1-HIRD (equivalent to SS1-TCRD) and twelve variables in SS2-HIRD (comparable to SS2-TCRD). In this configuration, the operating pressure on columns RD and C1 is set at 1.68 atm and 1 atm, respectively.

Based on the optimum design, the single and double side-stream flow rate in SS-HIRD was calculated to be eight and ten kmol/h, respectively. The configuration resembles SS-TCRD, wherein an ideal flow rate side stream results in a 90-94.5% reduction in the concentration of unreacted DMC within the recycle stream. The maintenance of a high purity level, namely at 99.5 mol%, for the DPC and MA products can be achieved by the support of conversion within the reaction zone of the RD column.

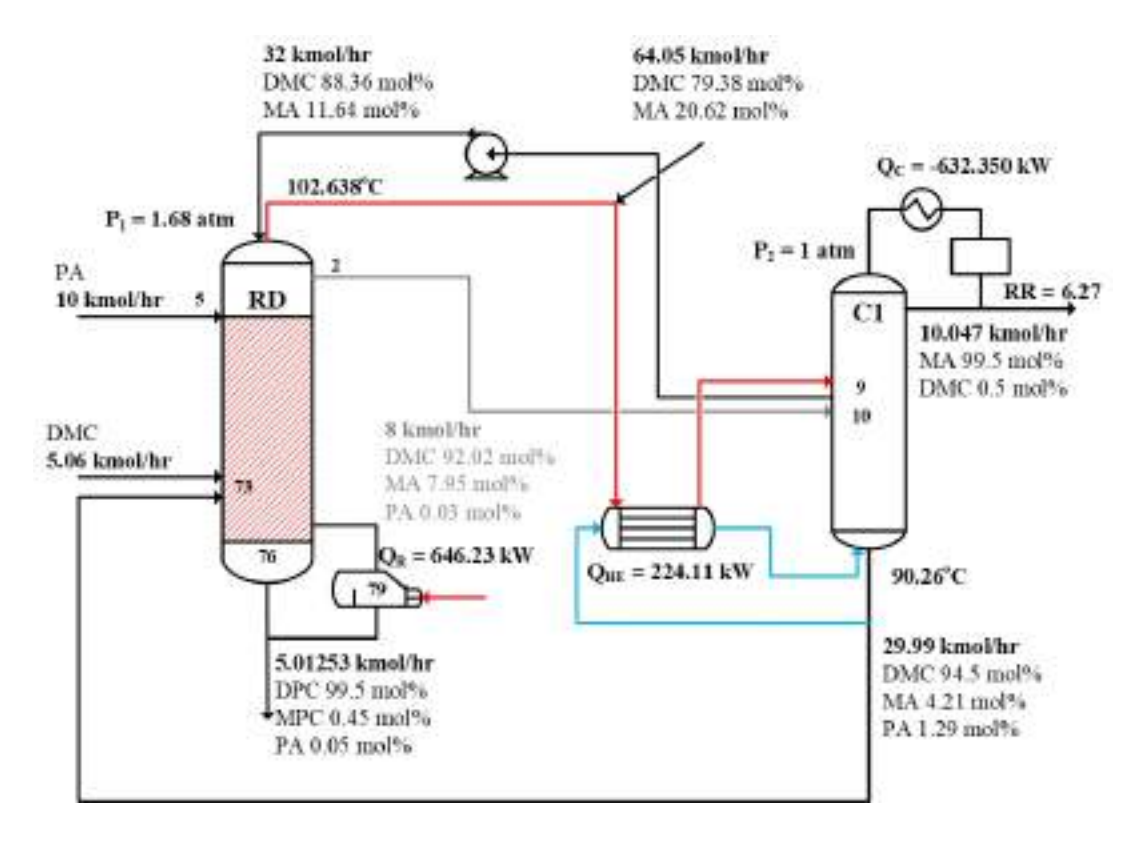


Figure 3. Result of optimum flowsheet for SS1-HIRD.

Figure 3 and 4 depicts the optimal configuration of SS1-HIRD and SS2-HIRD. The reboiler duty associated with column C1 has been eliminated and substituted with a heat exchanger (HE). This HE facilitates the transfer of latent heat from the top of the RD column to the bottom of column C1, providing the necessary heat to column C1. The HE energy usage in SS1-HIRD and SS2-HIRD are 224.11 kW and 236.22 kW. Therefore, the surface area of HE in SS1-HIRD and SS2-HIRD are measured to be 38.52 m² and 39.67 m², respectively. The HE employs a heat transfer coefficient of 0.568 kW/m2K, according to Luyben [32]. SS1-HIRD and SS2-HIRD can reduce energy consumption by up to 42.72 % and 47.27 %, respectively, and increase TAC savings by up to 28.46% and 31.46 %, respectively, as depicted in Table 1.

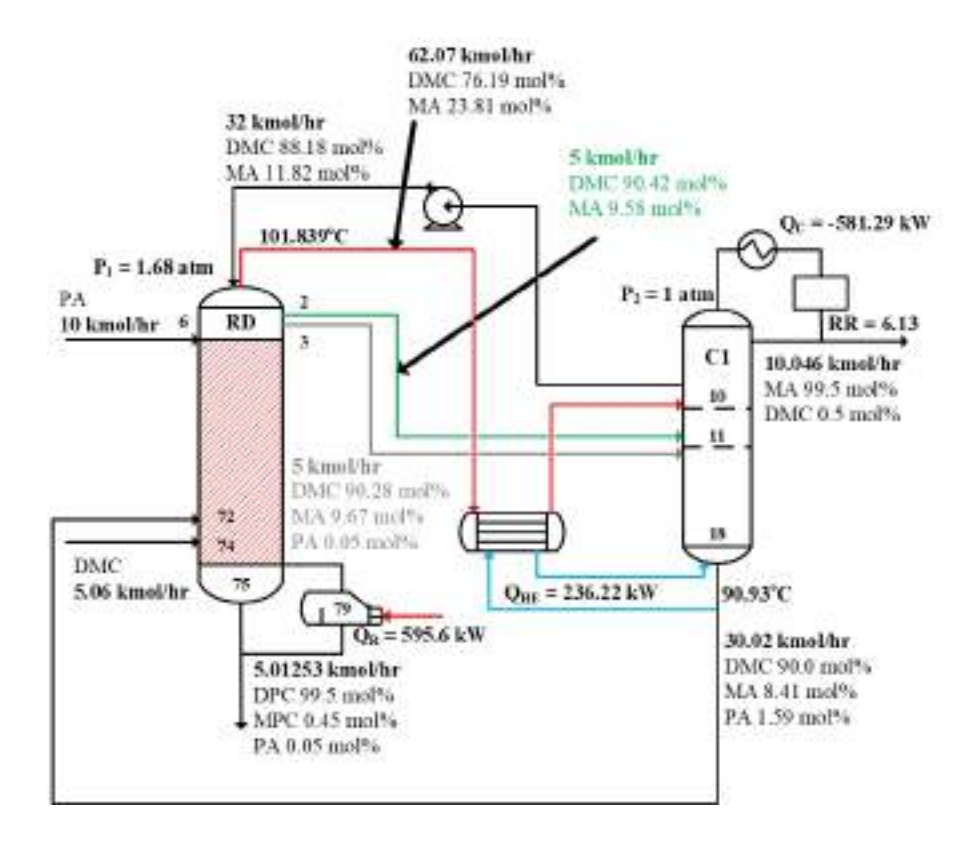


Figure 4. Result of optimum flowsheet for SS2-HIRD.

4.3 Results and discussion

Side-stream design benefits DPC production when combined with TCRD and HIRD, as evidenced by the evaluation of TAC reductions and energy usage. When doing a comparison, it can be observed that SS-HIRD exhibits a higher level of superiority than SS-TCRD. This assertion is grounded on the observation that, in the absence of side-streams, energy efficiency, and TAC savings, HIRD exhibits superiority over TCRD, as evidenced by the findings reported by Lee et al. [18]. The present investigation reveals a notable disparity in energy efficiency between SS-HIRD and SS-TCRD, with an average discrepancy of 16.78%. Furthermore, a disparity in TAC savings amounting to 5.78% was observed. Furthermore, it is seen that the efficacy of the side-stream is superior in the SS-

HIRD configuration compared to the SS-TCRD. Specifically, the double side stream in the SS-HIRD configuration exhibits a 7.83% reduction in energy consumption when compared to the single side-stream. On the contrary, the percentage of SS-TCRD is merely 1.1%. The disparity between the two options may be much more pronounced in the context of TAC savings. Among the four configurations that have been put forth, it is evident that the SS2-HIRD design stands out as the most ideal. This configuration exhibits significant TAC savings, amounting to 47.28%, and notable energy savings of 31.46%. Hence, this particular configuration was selected to assess the efficacy of dynamic and control strategies.

5. Dynamic simulation and control strategy for SS2-HIRD configuration

During the practical implementation, it is common for there to be a minor disruption in both the content and flow rate of the feed. Hence, developing a control system that ensures equipment safety and adherence to product standards is imperative. This section examines the feasibility of various control systems through dynamic simulation in Aspen Dynamics V.11. This action was necessary to identify an improved control framework to effectively manage safety equipment and ensure the production of high-quality products. The dynamic control structure will incorporate the SS2-HIRD. SS2-HIRD demonstrates greater economic competitiveness when considering the steady-state design outcomes.

5.1 Design of control loops

There are two designs of control loops: the quality control loop and the inventory control loop. Quality control measures were implemented to monitor and regulate the temperature and composition of the product, ensuring its purity. The inventory control encompassed monitoring the liquid level, flow rate, and pressure and was directly linked to maintaining the material balance of the process, ensuring process safety. In the present investigation, a temperature controller was employed to regulate the product specifications, as opposed to employing a composition controller.

This study proposes two inventory control loops (inventory A and B) to maintain the liquid level at the bottom of the C1 column (Sump C1) and ensure the safety and stability of the process. The difference between these inventories is in controlling the liquid level at the bottom of the second C1 column. Adjusting the liquid level controller in inventory A will increase the discharge from the bottom of the C1 column as the liquid level rises. Conversely, the release amount from the bottom of the C1 column is controlled proportionally to the amount of PA feed for Inventory B. In contrast, the liquid level at the bottom of the C1 column is governed by the fresh feed of DMC.

In SS2-HIRD, the reactant feed ratio (FR_{RD}) and the heat load of the reboiler in the RD column (QR_{RD}) can be employed as operating variables. The reflux ratio of the C1, RR_{C1}, controls the temperature in the C1 column. The temperature control points were selected using an open-loop sensitivity analysis, and the test results for open-loop sensitivity are shown in Figures S4 and S5 for the RD column and Figure S6 for the C1 column. Therefore, the temperature of the seventy-fourth stage was used as the temperature control point ($T_{74,RD}$) and controlled by QR_{RD} because it was more sensitive than the

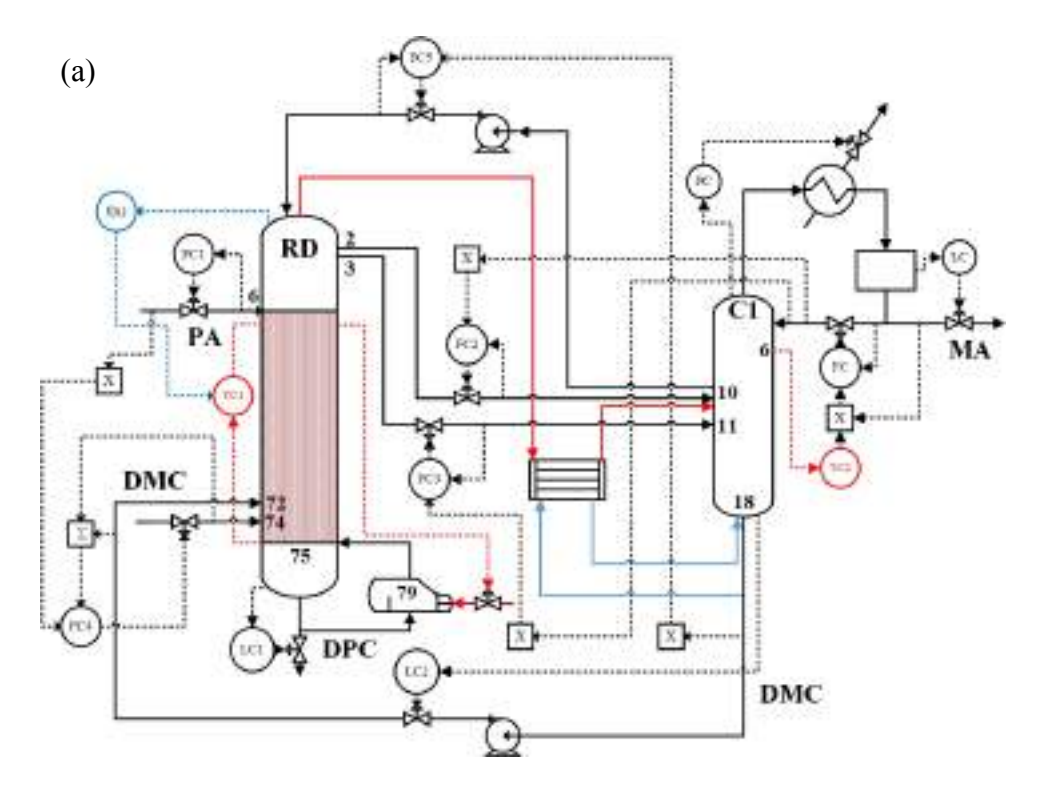
temperature of the forty-sixth stage ($T_{46,RD}$), and the location was closer to the two operating variables. In the C1 column, the sixth stage was chosen ($T_{6,C1}$). Because RR_{C1} is closer to the sensitive stages at the top of the column, it was used to maintain the temperature in the C1 column.

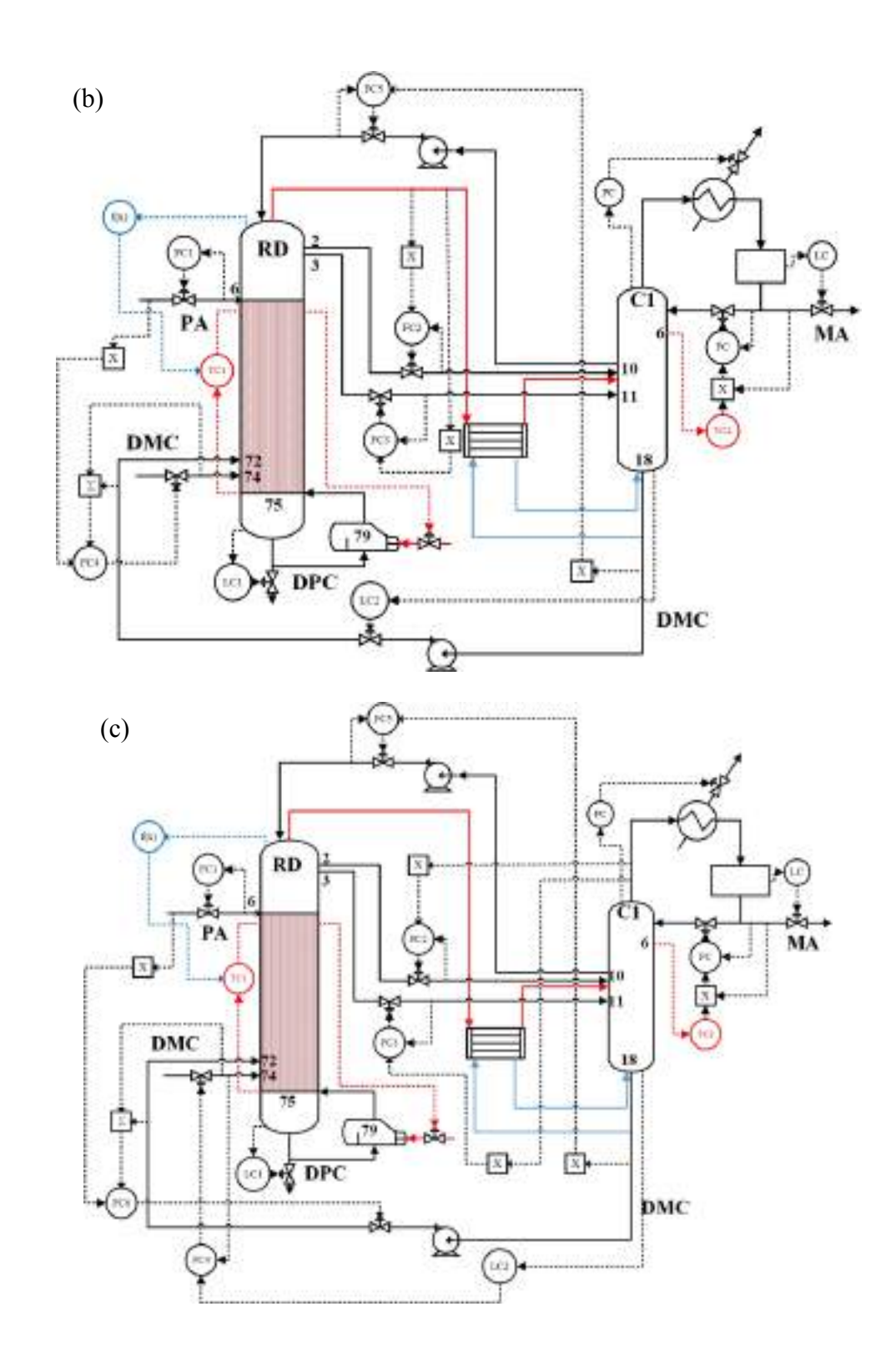
The SS2-HIRD control structure may cause the DPC product to deviate from the set value due to the inability to control the pressure in the RD column during heat integration, as conducted in our previous study without a side-stream [18]. This results in incorrect temperature values and changes in the product's composition. To address this, the ideal composition control loop for the pressure compensation temperature (PCT) controller was used to adjust the set point and test the relationship between the temperature set point and the top pressure of the RD column, as proposed by Luyben [35] and Yu et al. [36]. The results shown in Figure S7 demonstrated a linear relationship between the temperature set point and the pressure at the top of the RD column. When a disturbance occurred, the set point of the temperature controller for the RD column was adjusted in the dynamic simulation using the temperature change function acquired by regression. At the top of the RD column, the compensated control loop pressure was integrated with the temperature setpoint in the sensitive stage section. This maintains the set-point temperature at the stage, which is sensitive to changes in the upper pressure during disturbances.

The parameters of the two temperature controllers were established, and the simulation relay feedback test was performed using closed-loop auto-tune variation (ATV) methods. The test results were then input into the Tyreus-Luyben tuning rule to determine the controller parameters. Tables S3 and S4 show the parameters measured in all control structures.

5.2 Control structures and performances

Based on the different structures of the inventory and quality control loops, in this study, we proposed four control structures: control structure 1 (CS1), CS2, CS3, and CS4. In CS1 and CS2, inventory A is adopted. The QR_{RD} was used as a variable temperature manipulation to control $T_{74,RD}$. The fresh feed DMC must be maintained through the FR_{RD} by the temperature controller so that the number of components in the fresh feed DMC varies significantly at the beginning of the capacity adjustment. In CS1, owing to the addition of the side-stream flow rate, the two side-streams are rationed to RR_{C1}. In the context of CS2, a comparison was made between the side-stream's flow rate and the overhead vapor's distillation to regulate the side-stream flow. The CS1 and CS2 are shown in Figures 5a and b.





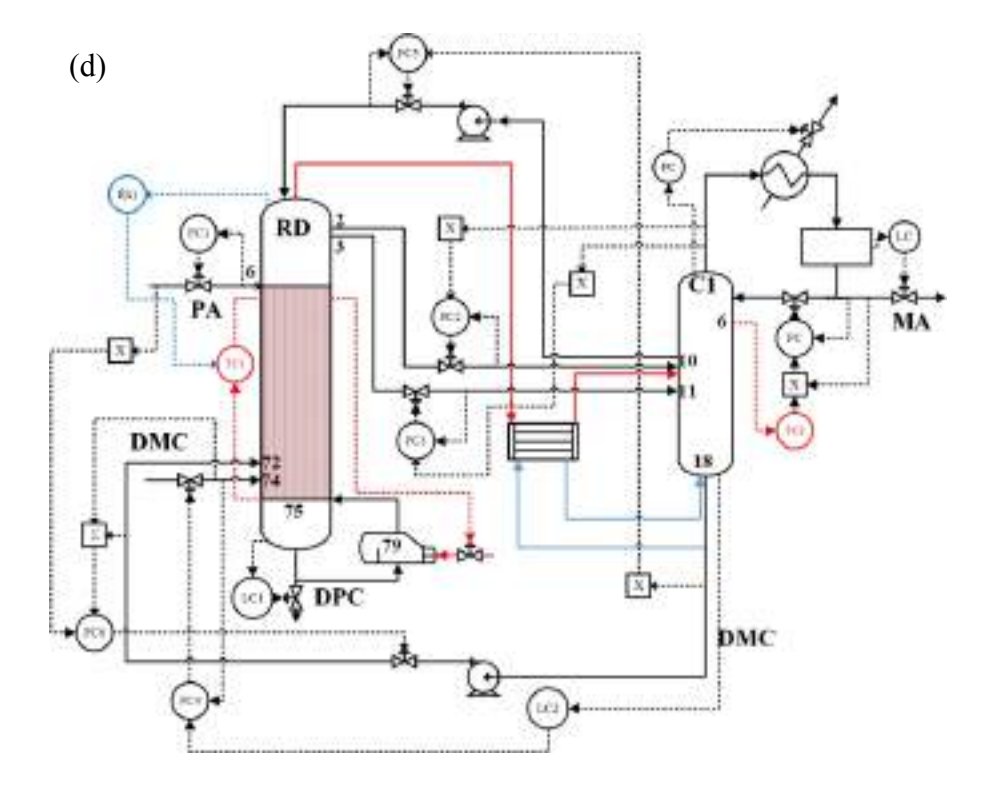
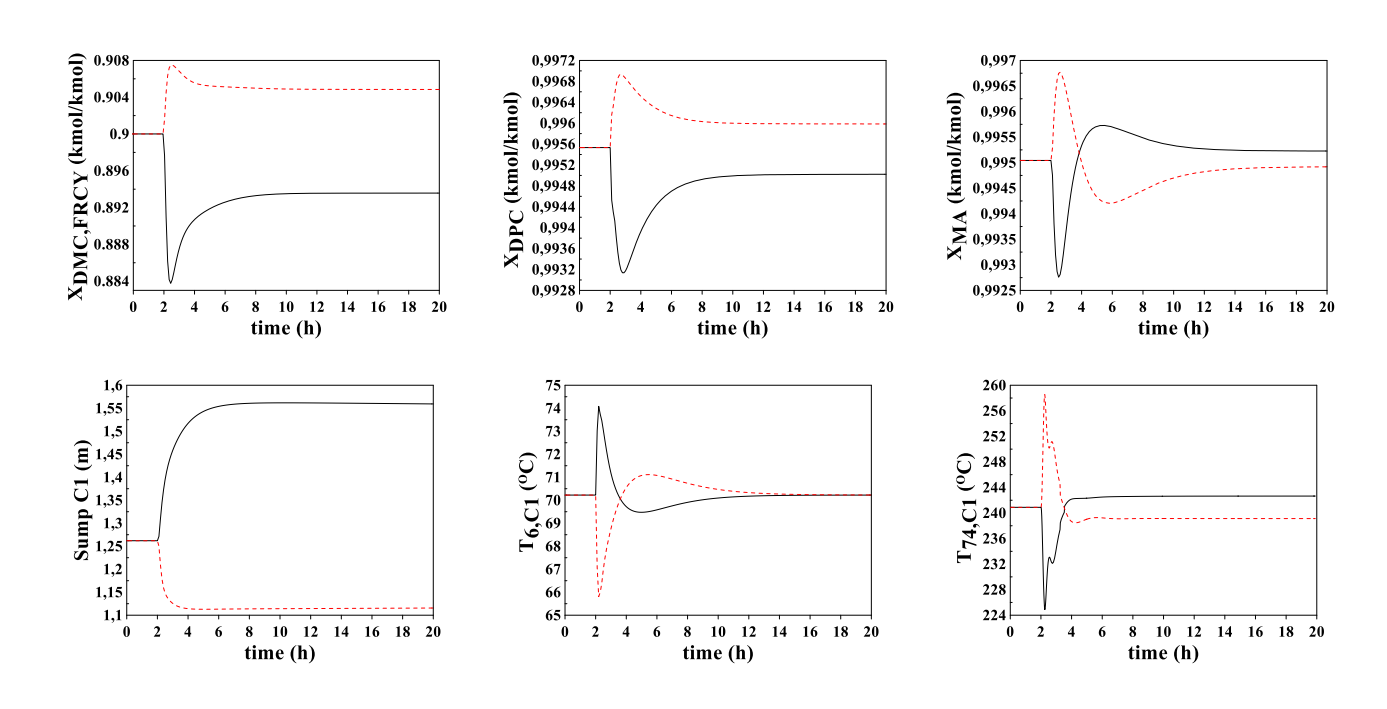


Figure 5. Scheme of CS1 (a), CS2 (b), CS3 (c), and CS4 (d).

In a broad sense, CS1 and CS2 exhibit nearly identical dynamic reactions due to their comparable control systems. Nevertheless, the extent to which the product response of CS2 exceeded expectations was significantly superior to that of CS1 (Figures 6 and 7). This comparison was made between the flow rate of the side-stream and the flow rate of the overhead vapor stream. During a feed disturbance, wherein the capacity experiences an increase, there is an impact on the flow rate of the overhead vapor stream that ascends to the upper section of the RD column. This alteration could modify the ratio between the flow rate at the top of the RD column and the flow rate of the side-stream. Comparing the side-stream flow rate to the overhead vapor stream enables the mitigation of disruptions that may occur during the process.

Based on the findings of the response CS1 and CS2, it can be inferred that FR_{RD}, specifically the fresh feed DMC, significantly impacts the transient change in the amount of DMC being fed. The flow rate of the fresh DMC exhibited a low magnitude, leading to a significant and abrupt transitory alteration. Furthermore, it can be observed that the lower liquid portion of the C1 column in both CS1 and CS2 exhibits a similar alteration in liquid level concomitant with an increase in production capacity. This phenomenon mainly arises due to utilizing the lower discharge of the C1 column in inventory A to regulate its liquid level. Consequently, inventory B was employed as the mechanism for inventory control in CS3 and CS4, as illustrated in Figures 5c and d. In addition to using inventory B, CS4 also incorporates the methodology employed in CS2, wherein the flow rate of the side-stream is adjusted to align with the flow rate of the overhead vapor stream.



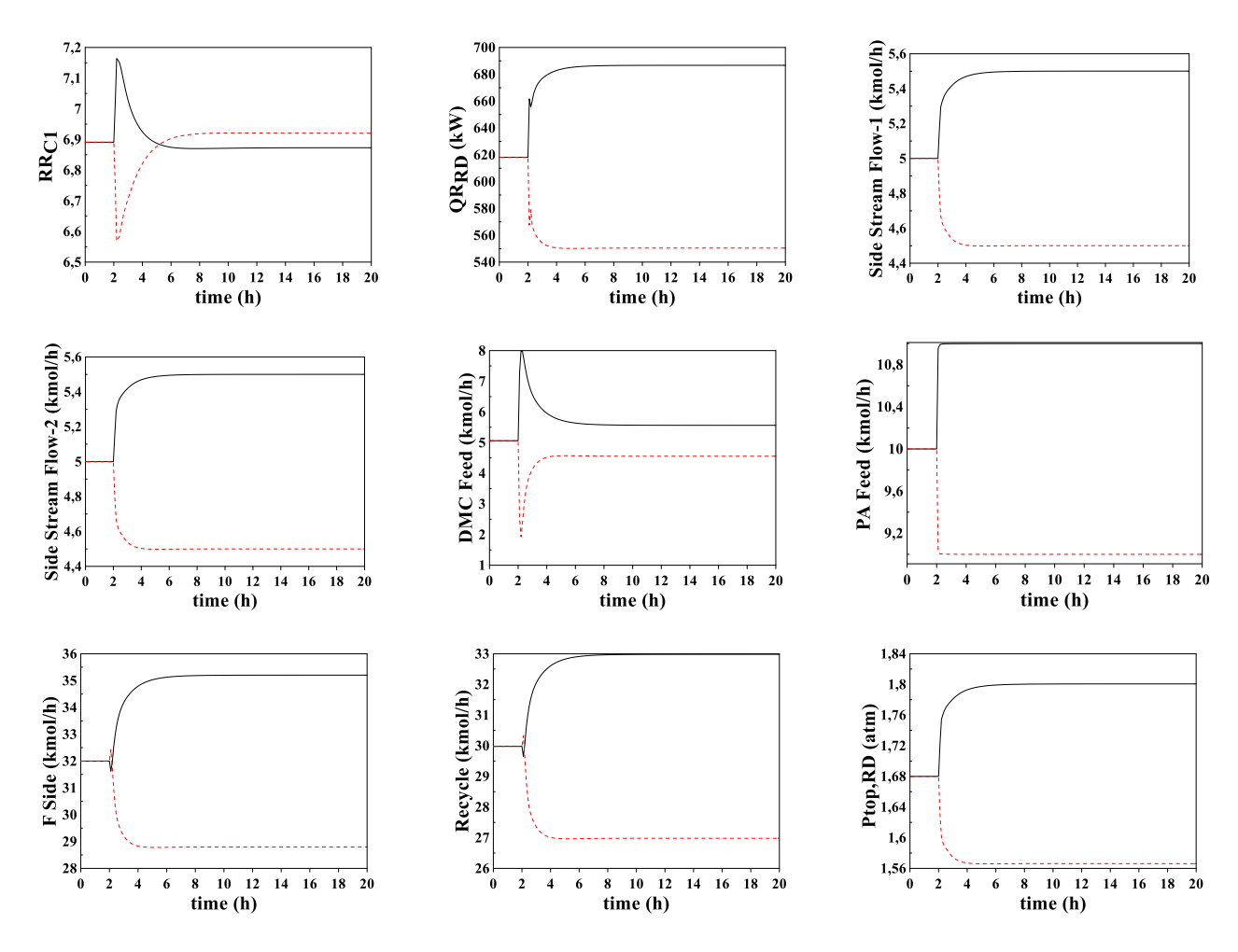
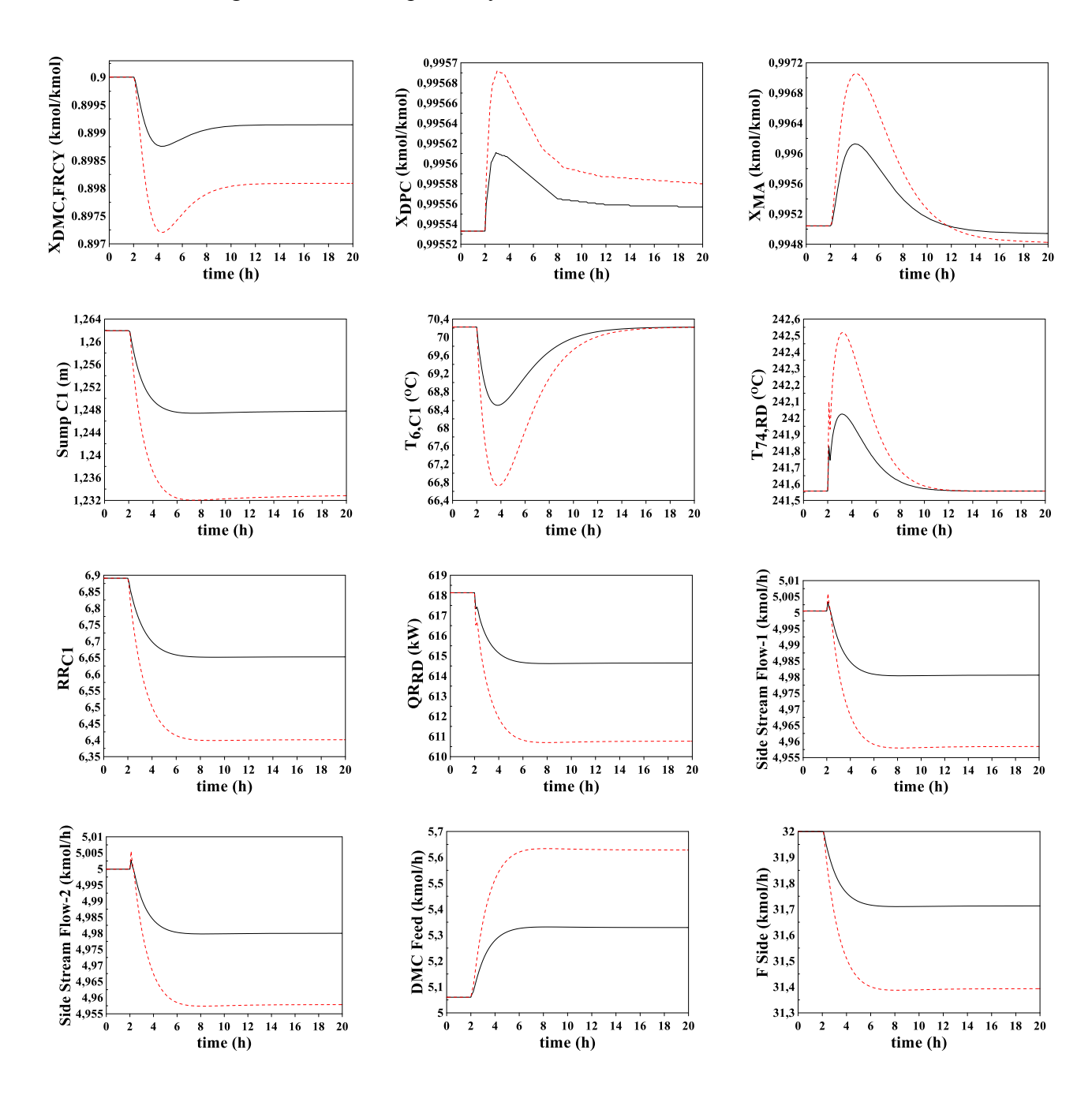
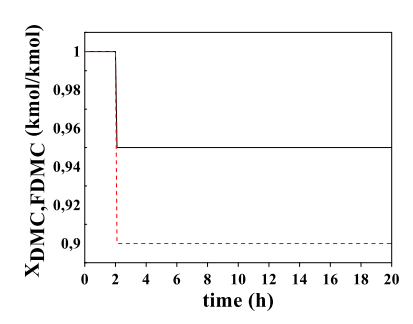


Figure 6. Responses to +10% (black straight line) and -10% (red dashed line) throughput disturbances for CS2.

CS3 performed the response outcomes according to feed throughput and composition profile disturbance, respectively (Figures S10 and S11). The findings indicate that implementing proportionate control of the DMC reflux flow rate and PA feed is a good strategy for mitigating the effects of the throughput disturbance test. Furthermore, utilizing fresh feed DMC to regulate the liquid bottom level of the C1 column can effectively overcome the throughput disturbance test. Moreover, the utilization of inventory B results in a diminished effect of the disturbance test on both the liquid bottom level of the C1 column and the recycle flow of DMC, compared to inventory A. On the other hand, CS4,

with the ratio of the flow rate of the side-stream and the flow rate of the overhead vapor stream, reveals a potential reduction in product purity overshoot during disturbances, as illustrated in Figures 8 and 9, respectively.





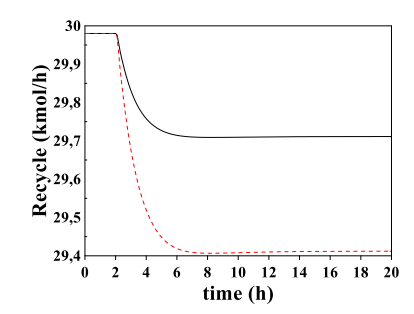
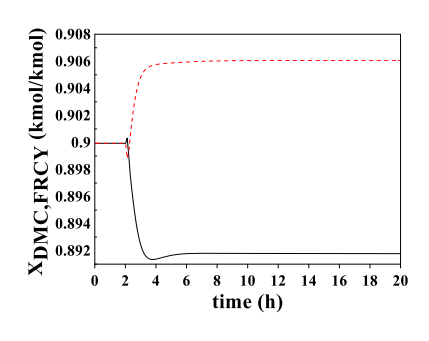
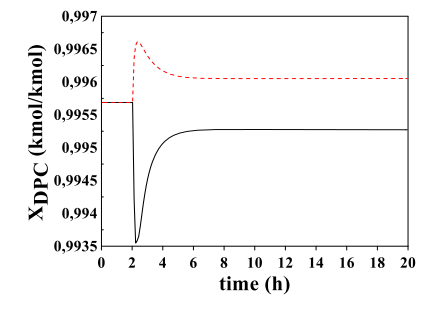
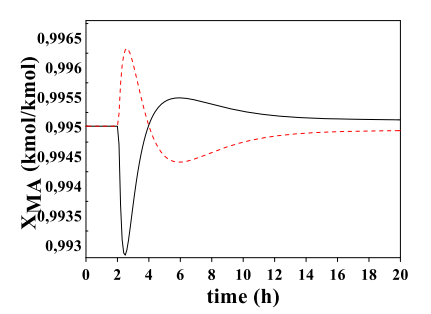


Figure 7. Responses to 5% (black straight line) and 10% (red dashed line) composition disturbance for CS2.

The outcomes achieved in the suggested structural control strategy, specifically CS1, CS2, CS3, and CS4, exhibited encouraging findings in preserving the integrity of the DPC substances. Hence, an Integral Absolute Error (IAE) is essential for optimal performance in the suggested structural control scheme. The IAE formulation calculates the percentage error between the input and preset set-point values. The Aspen Dynamic involves utilizing the IAE metric to assess the performance of a control system in maintaining a process variable at its designated set point (SP) throughout the whole dynamic response of the controlled process. The set point can be established within the block itself or obtained as input from another block.







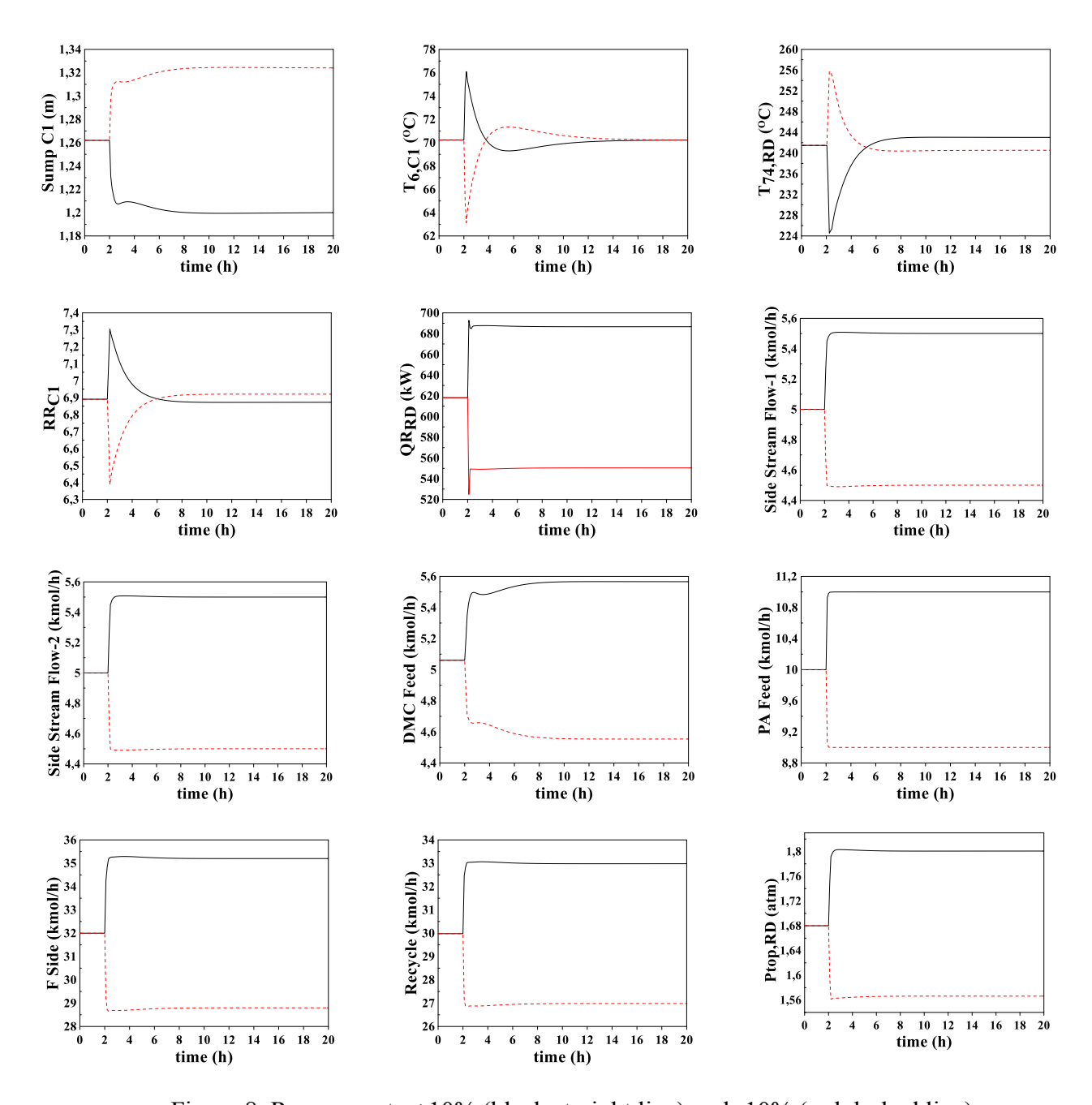
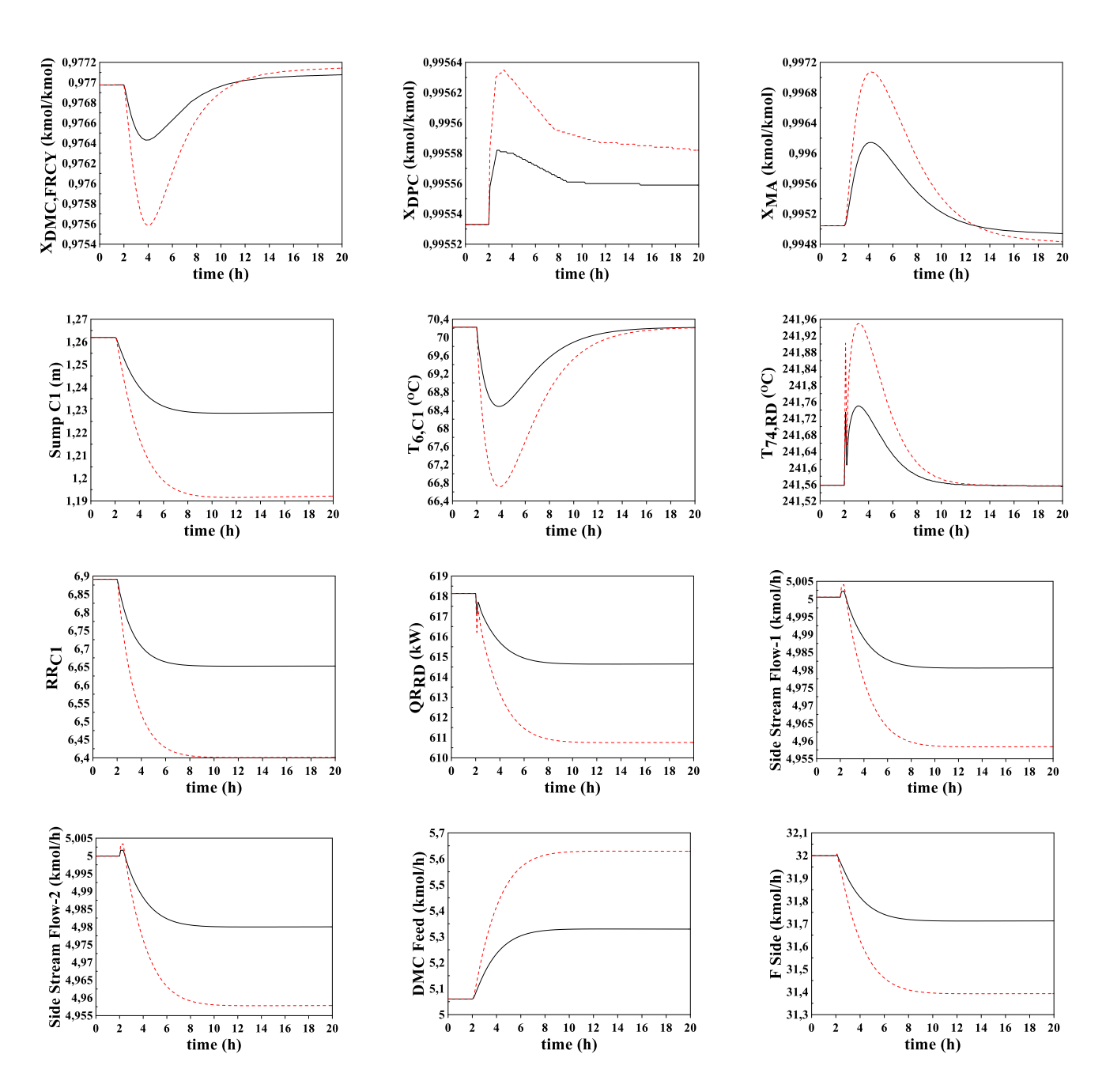
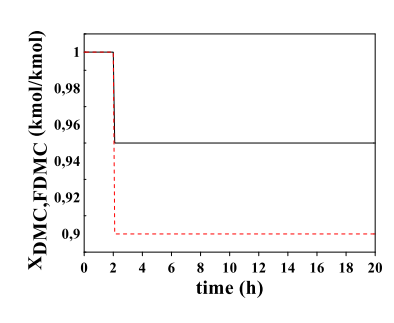


Figure 8. Responses to +10% (black straight line) and -10% (red dashed line) throughput disturbances for CS4.

The findings for the IAE between CS2, CS3, and CS4 are presented in Table 2. The utilization of fresh feed DMC was employed to regulate the feed ratio. However, it was observed that this approach resulted in overshooting when there were interruptions in

throughput in CS1 and CS2. This phenomenon can be attributed to DMC's relatively low fresh feed flow rate. Furthermore, the lowermost tier of the C1 column exhibits a gradual increment before attaining a condition of equilibrium. This phenomenon is because the flow rate at the bottom of column C1 regulates the liquid level in column C1. Hence, it is not advisable to pursue CS1 and CS2.





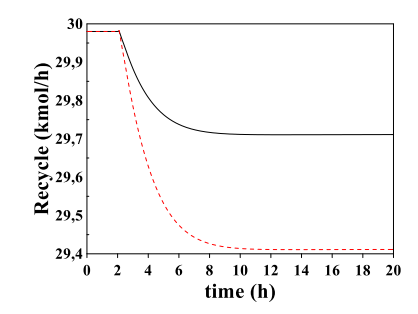


Figure 9. Responses to 5% (black straight line) and 10% (red dashed line) composition disturbance for CS4.

The inventory B scheme could address the challenges encountered in the CS1 and CS2 schemes within the context of CS3 and CS4. Moreover, it is worth noting that the control structure implemented in CS4 exhibits the lowest value of IAE. This indicates that the control system effectively preserves the integrity of the DPC and ensures that the MA closely aligns with the desired set point value. The values of IAE in the field of CS4 are $\pm 10\%$ for feed disturbance at a DPC of 0.001% and 0.002% and $\pm 10\%$ for feed disturbance at an MA of 0.06% and 0.0015, respectively. The composition disturbances at the DPC are within a range of $\pm 5\%$, with values of 0.0005% and 0.001%. Similarly, the composition disturbances at the MA are within a range of $\pm 10\%$, with values of 0.0033% and 0.0067%, respectively. Hence, the control structure of CS4 exhibits enhanced performance in ensuring the safety and maintaining the quality of the process.

Table 2. Results summary of IAE.

		CS3		CS2		CS4	
		DPC (%)	MA (%)	DPC (%)	MA (%)	DPC (%)	MA (%)
Feed	+10%	0.021	0.0072	0.0117	0.0062	0.001	0.06
Disturbance	-10%	0.098	0.0068	0.0095	0.0059	0.002	0.0015
Composition	+5%	0.0014	0.0047	0.00057	0.0038	0.0005	0.0033
Disturbance	+10%	0.0023	0.0081	0.0012	0.0076	0.001	0.0067

6. Conclusion

Based on the analysis of four proposed designs: SS1-TCRD, SS2-TCRD, SS1-HIRD, and SS2-HIRD; adding a side-stream configuration to developing a TCRD and HIRD can reduce energy consumption and save the TAC compared to conventional RD. The most advantageous proposed design is the SS2-HIRD. It can increase the TAC savings and decrease the reboiler duty in operation by up to 47.27 % and 31.46%, respectively, compared to conventional RD.

SS2-HIRD's dynamic control structure performance is also investigated. CS4, which uses inventory B and rationing the flow rate side-stream with the overhead vapor stream, shows the best response to overcome the 10% throughput change and 5-10% mole composition disturbance. Compared to other control structures, the CS4 has the lowest IAE value. The purity of DPC and MA was set for IAE to see the error percentage from the set value when the disturbance occurred. The IAE values in CS4 are $\pm 10\%$ feed disturbance at DPC 0.001% and 0.002, $\pm 10\%$ feed disturbance at MA 0.06% and 0.0015. $\pm 5\%$ composition disturbance at DPC 0.0005% and 0.001%, $\pm 10\%$ composition disturbance at MA 0.0033% and 0.0067%.

CRediT authorship contribution statement

Bangkit Gotama: Writing-original draft, Writing-review and editing. **Tua Halomoan**: Conceptualization, Methodology, Investigation, Writing-original draft. **Yu-Ying Chen**: Writing-review and editing. **Hao-Yeh Lee**: Conceptualization, Writing-review and editing, Supervision, Project administration, Funding acquisition.

Declaration of competing interest

The authors declare that they have no known competing financial interests or personal relationships that could have appeared to influence the work reported in this paper.

Acknowledgments

This work was supported by the Ministry of Science and Technology of Taiwan under grant MOST 111-2221-E-011 -003 -, which is gratefully acknowledged.

References

- [1] M. Gohil and G. Joshi, "Perspective of polycarbonate composites and blends properties, applications, and future development: A review," *Green Sustainable Process for Chemical and Environmental Engineering and Science: Green Composites: Preparation, Properties and Allied Applications*, pp. 393–424, 2022, doi: 10.1016/B978-0-323-99643-3.00012-7.
- [2] S. Fukuoka, I. Fukawa, T. Adachi, H. Fujita, N. Sugiyama, and T. Sawa, "Industrialization and expansion of green sustainable chemical process: A Review of Non-phosgene Polycarbonate from CO2," *Org Process Res Dev*, vol. 23, no. 2, pp. 145–169, 2019, doi: 10.1021/acs.oprd.8b00391.
- [3] W. B. Kim, U. A. Joshi, and J. S. Lee, "Making Polycarbonates without Employing Phosgene: An Overview on Catalytic Chemistry of Intermediate and Precursor Syntheses for Polycarbonate," *Industrial and Engineering Chemistry Research43*, vol. 43, no. 9, pp. 1897–1914, 2004, doi: 10.1021/ie034004z.
- [4] J. Gong, X. Ma, and S. Wang, "Phosgene-free approaches to catalytic synthesis of diphenyl carbonate and its intermediates," *Appl Catal A Gen*, vol. 316, no. 1, pp. 1–21, 2007, doi: 10.1016/J.APCATA.2006.09.006.
- [5] P. Cao *et al.*, "Molybdenum Trioxide Catalyst for Transesterification of Dimethyl Carbonate and Phenyl Acetate to Diphenyl Carbonate," *Chinese Journal of Catalysis*, vol. 30, no. 9, pp. 853–855, 2009, doi: 10.1016/S1872-2067(08)60127-8.
- [6] L. Ying and H. Shunwu, "Study on MoO 3 /SBA-16 catalyzed transesterification to synthesize diphenyl carbonate," *Turk J Chem*, vol. 46, pp. 1930–1945, 2022, doi: 10.55730/1300-0527.3492.

- [7] K. Cheng, S. J. Wang, and D. S. H. Wong, "Steady-state design of thermally coupled reactive distillation process for the synthesis of diphenyl carbonate," *Comput Chem Eng*, vol. 52, pp. 262–271, 2013, doi: 10.1016/J.COMPCHEMENG.2013.02.001.
- [8] H. Y. Ho, S. S. Shu, S. J. Wang, and M. J. Lee, "Isothermal (vapour + liquid) equilibrium (VLE) for binary mixtures containing diethyl carbonate, phenyl acetate, diphenyl carbonate, or ethyl acetate," *J Chem Thermodyn*, vol. 91, pp. 35–42, 2015, doi: 10.1016/J.JCT.2015.07.024.
- [9] Z. Jiang and R. Agrawal, "Process intensification in multicomponent distillation: A review of recent advancements," *Chemical Engineering Research and Design*, vol. 147, pp. 122–145, 2019, doi: 10.1016/J.CHERD.2019.04.023.
- [10] A. K. Tula, M. R. Eden, and R. Gani, "Computer-aided process intensification: Challenges, trends and opportunities," *AIChE Journal*, vol. 66:e16819, 2019, doi: 10.1002/aic.16819.
- [11] Z. Y. Kong, E. Sánchez-Ramírez, A. Yang, W. Shen, J. G. Segovia-Hernández, and J. Sunarso, "Process intensification from conventional to advanced distillations: Past, present, and future," *Chemical Engineering Research and Design*, vol. 188, pp. 378–392, 2022, doi: 10.1016/J.CHERD.2022.09.056.
- [12] J. G. Segovia-Hernández, S. Hernández, and A. Bonilla Petriciolet, "Reactive distillation: A review of optimal design using deterministic and stochastic techniques," Chemical Engineering and Processing: Process Intensification, vol. 97, pp. 134–143, 2015, doi: 10.1016/J.CEP.2015.09.004.
- [13] H. Y. Lee, S. Y. Li, and C. L. Chen, "Evolutional Design and Control of the Equilibrium-Limited Ethyl Acetate Process via Reactive Distillation-Pervaporation

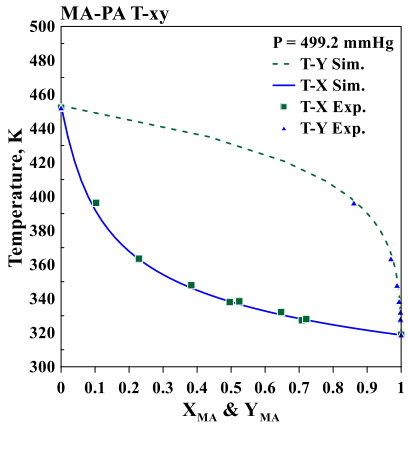
- Hybrid Configuration," *Ind Eng Chem Res*, vol. 55, no. 32, pp. 8802–8817, 2016, doi: 10.1021/acs.iecr.6b01358.
- [14] X. Pei, H. Li, Z. Zhang, Y. Meng, X. Li, and X. Gao, "Process intensification for energy efficient reactive distillation of trioxane production from aqueous formaldehyde," *Chemical Engineering and Processing Process Intensification*, vol. 175, p. 108914, 2022, doi: 10.1016/J.CEP.2022.108914.
- [15] I. Pazmiñ O-Mayorga, M. Jobson, and A. A. Kiss, "A Systematic Methodology for the Synthesis of Advanced Reactive Distillation Technologies," *Ind Eng Chem Res*, vol. 62, no. 14, pp. 5907–5928, 2023, doi: 10.1021/acs.iecr.2c04540.
- [16] J. R. Alcántara-Avila, M. Terasaki, H. Y. Lee, J. L. Chen, K. I. Sotowa, and T. Horikawa, "Design and control of reactive distillation sequences with heat-integrated stages to produce diphenyl carbonate," *Ind Eng Chem Res*, vol. 56, no. 1, pp. 250–260, 2017, doi: 10.1021/acs.iecr.6b02651.
- [17] H. Y. Lee *et al.*, "Design and control of diphenyl carbonate reactive distillation process with thermally coupled and heat-integrated stages configuration," *Comput Chem Eng*, vol. 121, pp. 130–147, 2019, doi: 10.1016/j.compchemeng.2018.10.009.
- [18] H. Y. Lee, F. J. Novita, and K. C. Weng, "Hybrid heat-integrated design and control for a diphenyl carbonate reactive distillation process," *Chemical Engineering and Processing Process Intensification*, vol. 162, p. 108344, 2021, doi: 10.1016/J.CEP.2021.108344.
- [19] G. Contreras-Zarazúa, J. A. Vázquez-Castillo, C. Ramírez-Márquez, G. A. Pontis, J. G. Segovia-Hernández, and J. R. Alcántara-Ávila, "Comparison of intensified reactive

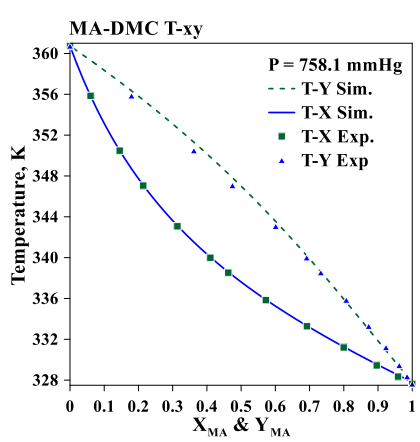
- distillation configurations for the synthesis of diphenyl carbonate," *Energy*, vol. 135, pp. 637–649, 2017, doi: 10.1016/J.ENERGY.2017.06.156.
- [20] G. Contreras-Zarazúa, E. Villicaña-García, B. Cansino-Loeza, J. A. Vázquez-Castillo, J. M. Ponce-Ortega, and J. G. Segovia-Hernández, "Environmental impact and occupational hazard evaluation on intensified processes to produce diphenyl carbonate," *Comput Chem Eng*, vol. 122, pp. 19–30, 2019, doi: 10.1016/J.COMPCHEMENG.2018.05.017.
- [21] G. Contreras-Zarazúa, J. A. Vázquez-Castillo, C. Ramírez-Márquez, J. G. Segovia-Hernández, and J. R. Alcántara-Ávila, "Multi-objective optimization involving cost and control properties in reactive distillation processes to produce diphenyl carbonate," *Comput Chem Eng*, vol. 105, pp. 185–196, 2017, doi: 10.1016/j.compchemeng.2016.11.022.
- [22] N. Yu, L. Li, M. Chen, J. Wang, D. Liu, and L. Sun, "Novel reactive distillation process with two side streams for dimethyl adipate production," *Chemical Engineering and Processing: Process Intensification*, vol. 118, pp. 9–18, 2017, doi: 10.1016/J.CEP.2017.04.010.
- [23] N. Van Duc Long and M. Lee, "Economical retrofit of reactive distillation with a total reflux design or a total boil-up design," *Chemical Engineering Research and Design*, vol. 145, pp. 53–63, 2019, doi: 10.1016/J.CHERD.2019.02.042.
- [24] Z. Y. Kong, G. C. Zarazúa, H. Y. Lee, J. Chua, J. G. Segovia-Hernández, and J. Sunarso, "Design of novel side-stream hybrid reactive-extractive distillation for sustainable ternary separation of THF/ethanol/water using mixed entrainer," *Process*

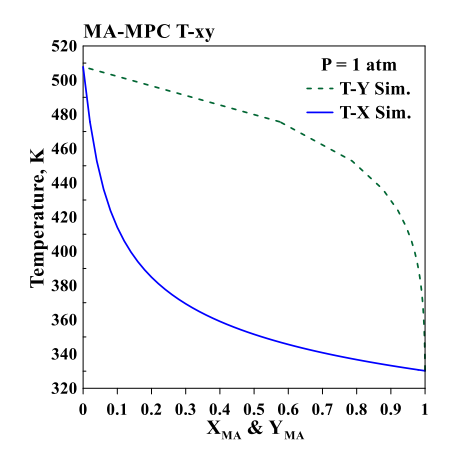
- Safety and Environmental Protection, vol. 166, pp. 574–588, 2022, doi: 10.1016/J.PSEP.2022.08.056.
- [25] A. Yang, Z. Y. Kong, and J. Sunarso, "Design and optimisation of novel hybrid side-stream reactive-extractive distillation for recovery of isopropyl alcohol and ethyl acetate from wastewater," *Chemical Engineering Journal*, vol. 451, p. 138563, 2023, doi: 10.1016/J.CEJ.2022.138563.
- [26] Q. Zhang, A. Zeng, X. Yuan, and Y. Ma, "Design and control of economically attractive side-stream extractive distillation process," *Chemical Engineering Research and Design*, vol. 160, pp. 571–586, 2020, doi: 10.1016/J.CHERD.2020.04.041.
- [27] J. Liu, X. Liu, J. Li, J. Ren, J. Wang, and L. Sun, "Design and control of side-stream extractive distillation to separate acetic acid and cyclohexanone from wastewater by varying pressure," *Process Safety and Environmental Protection*, vol. 159, pp. 1127–1149, 2022, doi: 10.1016/J.PSEP.2022.01.064.
- [28] Z. Zhang, X. Shi, X. Zhu, M. Li, and J. Gao, "Investigation of energy-saving thermally coupled extractive distillation alternatives with different liquid side-stream for a quaternary azeotropic system," *Sep Purif Technol*, vol. 268, p. 118706, 2021, doi: 10.1016/J.SEPPUR.2021.118706.
- [29] Z. Y. Yang, B. Y. Yu, and I. L. Chien, "An environmentally benign, energy intensified single-column side stream extractive distillation (SC-SSED) process for Acetone/n-heptane separation," *J Taiwan Inst Chem Eng*, vol. 149, p. 105018, 2023, doi: 10.1016/J.JTICE.2023.105018.
- [30] C. Cui, X. Zhang, and J. Sun, "Design and optimization of energy-efficient liquidonly side-stream distillation configurations using a stochastic algorithm," *Chemical*

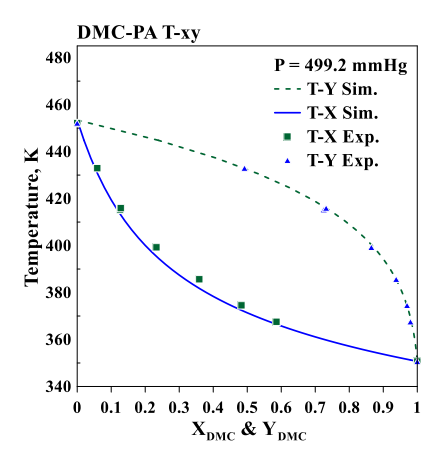
- Engineering Research and Design, vol. 145, pp. 48–52, 2019, doi: 10.1016/J.CHERD.2019.03.001.
- [31] C. Cui, Q. Zhang, X. Zhang, and J. Sun, "Eliminating the vapor split in dividing wall columns through controllable double liquid-only side-stream distillation configuration," *Sep Purif Technol*, vol. 242, p. 116837, 2020, doi: 10.1016/J.SEPPUR.2020.116837.
- [32] W. L. Luyben, *Distillation Design and Control Using Aspen Simulation*, Second. New Jersey: John Wiley & Sons, 2013.
- [33] C. T. Yao, "VLE and boiling point of binary system of methyl acetate, dimethyl carbonate, phenyl acetate and diphenyl carbonate," I-Shou University, Kaohsiung, 2012.
- [34] M. F. Cardoso, R. L. Salcedo, S. F. De Azevedo, and D. Barbosa, "Optimization of reactive distillation processes with simulated annealing," *Chem Eng Sci*, vol. 55, no. 21, pp. 5059–5078, 2000, doi: 10.1016/S0009-2509(00)00119-6.
- [35] W. L. Luyben, "Design and Control of a Fully Heat-Integrated Pressure-Swing Azeotropic Distillation System," *Ind Eng Chem Res*, vol. 47, no. 8, pp. 2681–2695, 2008, doi: 10.1021/ie0713660.
- [36] B. Yu, Q. Wang, and C. Xu, "Design and control of distillation system for methylal/methanol separation. Part 2: Pressure swing distillation with full heat integration," *Ind Eng Chem Res*, vol. 51, no. 3, pp. 1293–1310, 2012, doi: 10.1021/ie201949q.

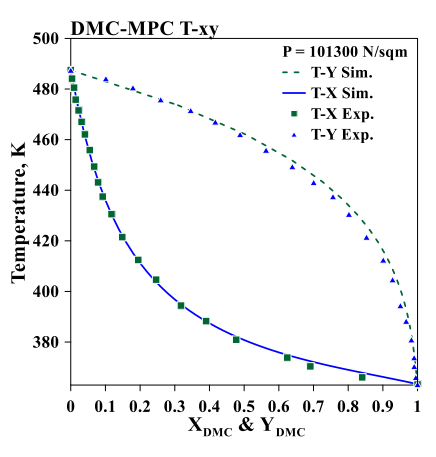
Supplementary Data – Figures

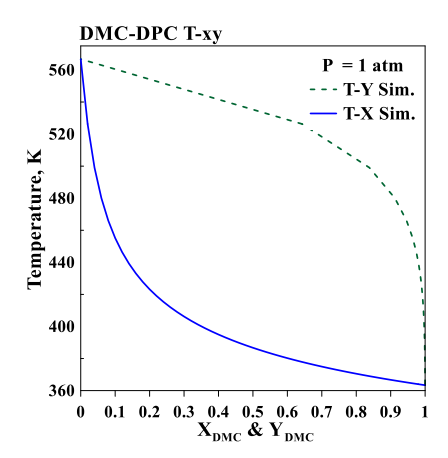












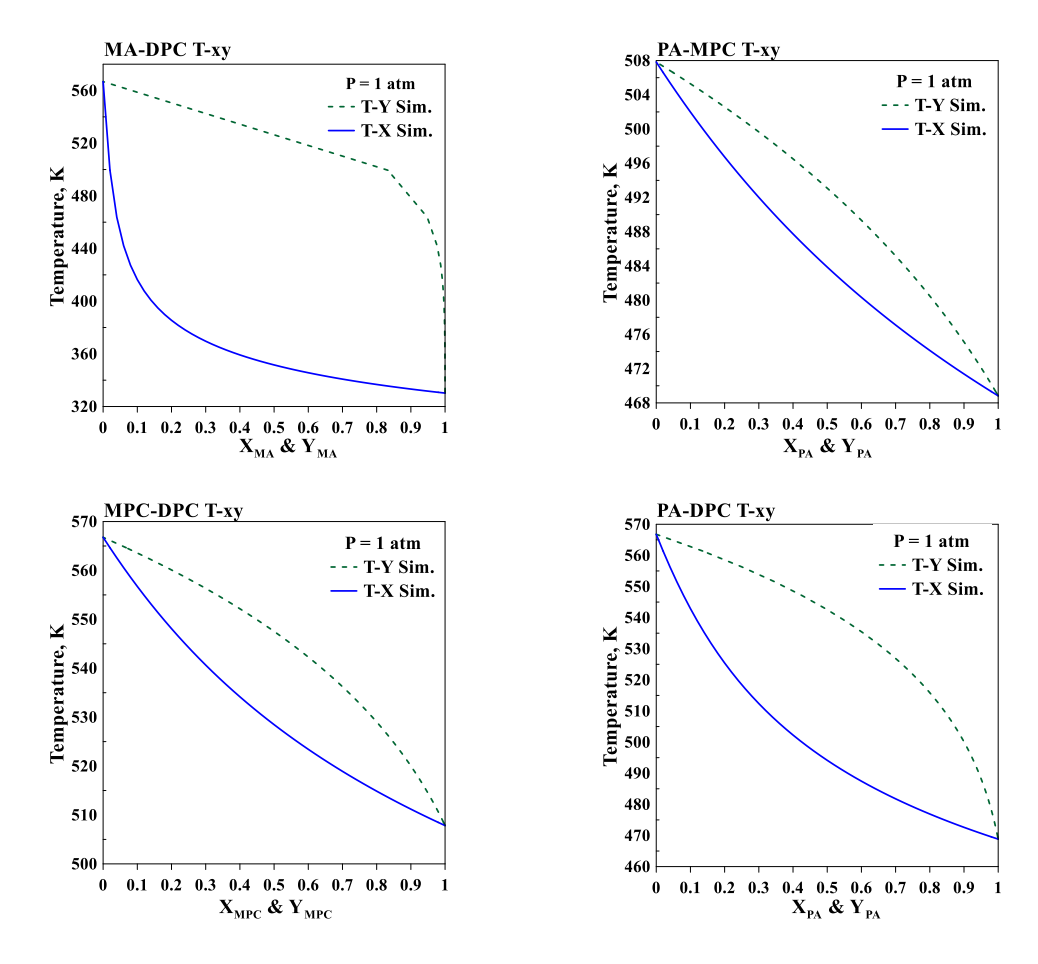


Figure S.1 T – xy diagram of each component in the DPC process.

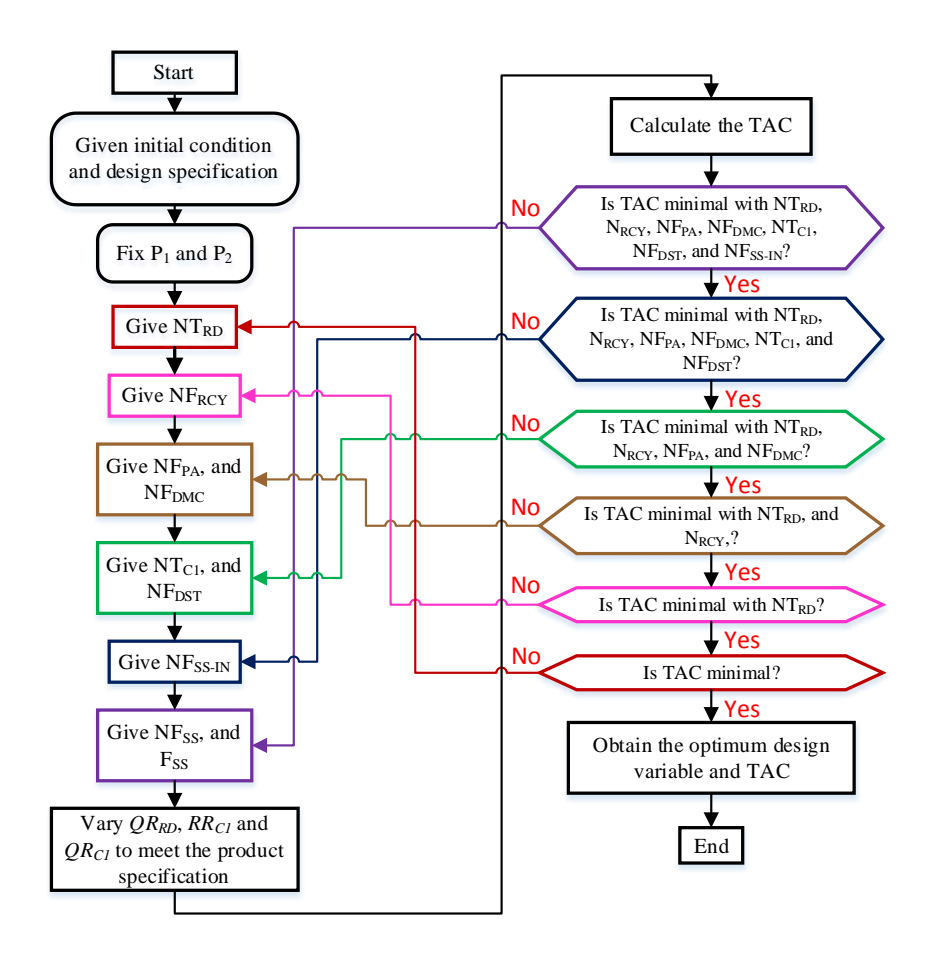


Figure S2. Sequential iterative optimization procedure for SS1-TCRD and SS1-HIRD.

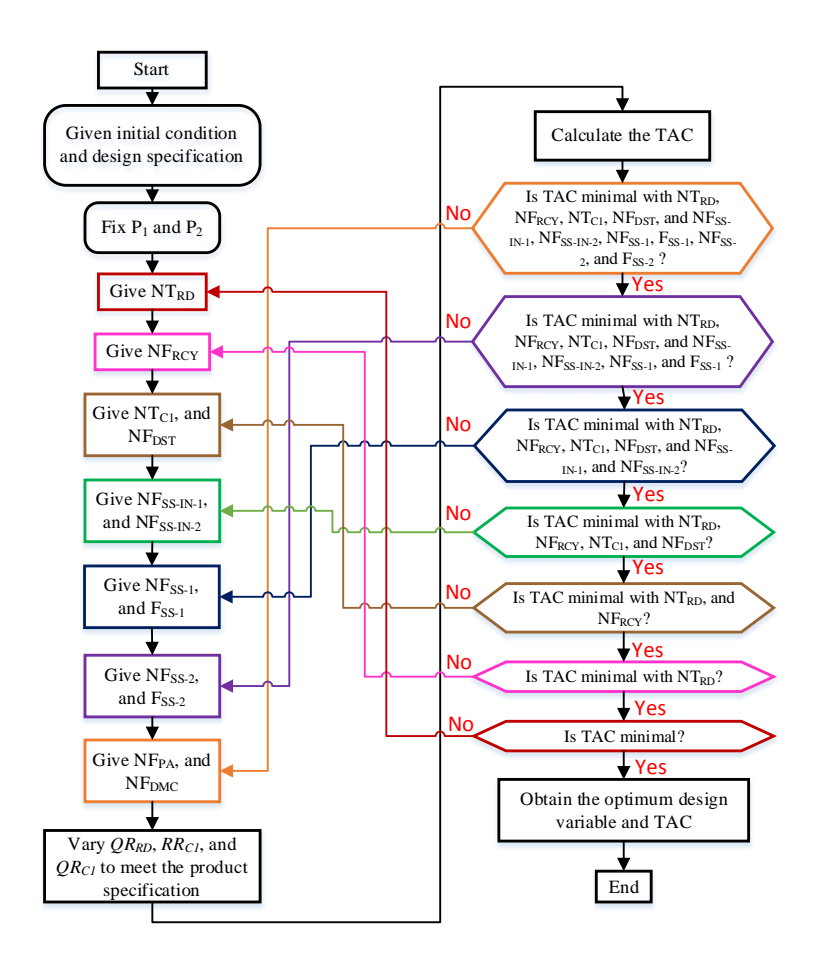


Figure S3. Sequential iterative optimization procedure for SS2-TCRD and SS2-HIRD.

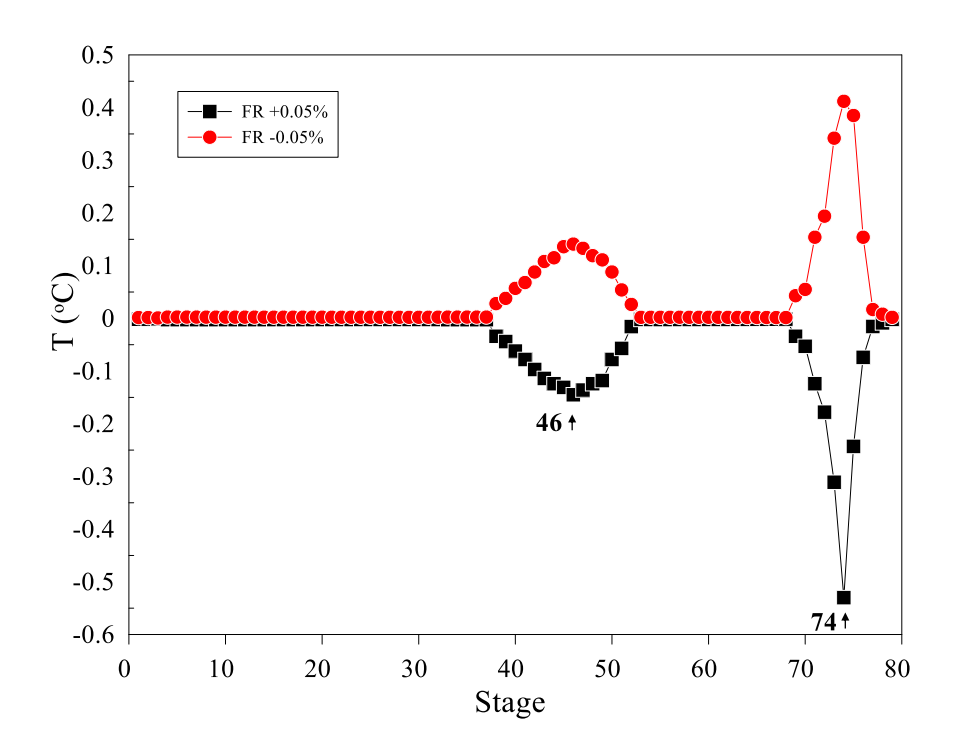


Figure S4. Open-loop sensitivity analysis of FR_{RD} \pm 0.05%.

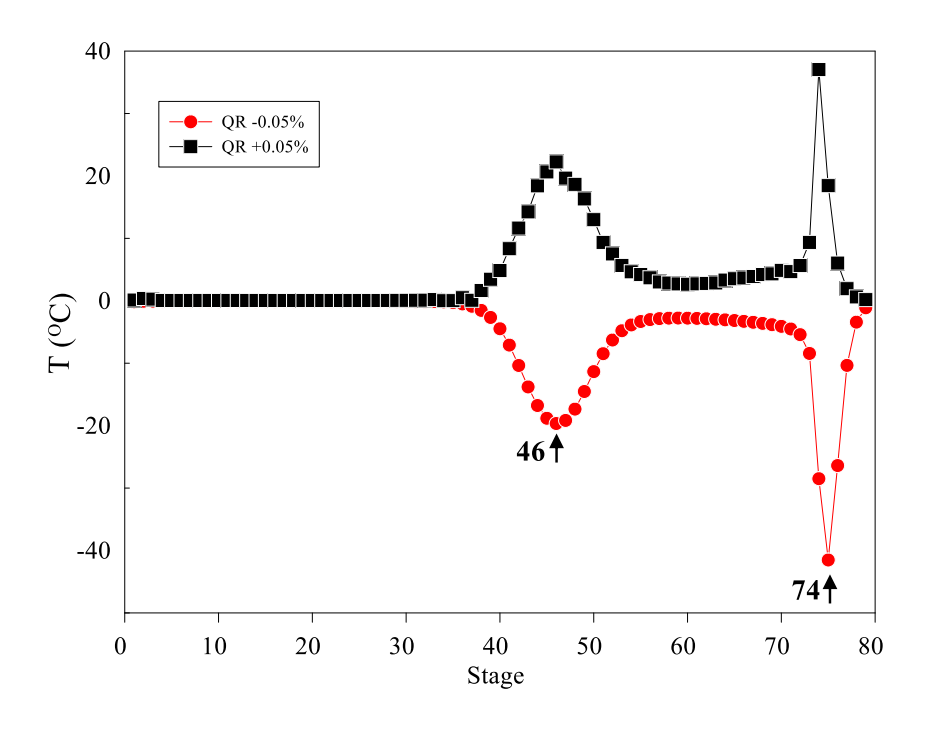


Figure S5. Open-loop sensitivity analysis of QR_{RD} \pm 0.05%.

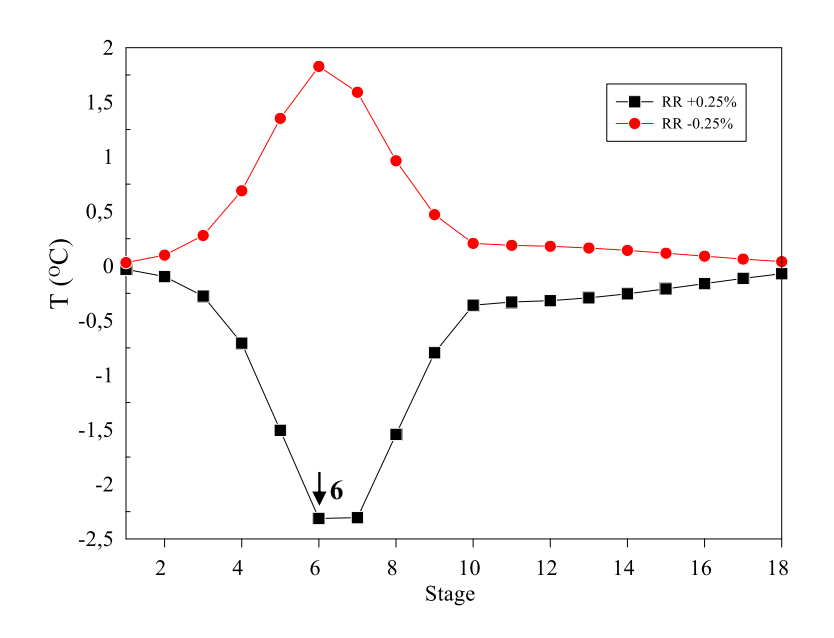


Figure S6. Open-loop sensitivity analysis of RR_{C1} \pm 0.25%.

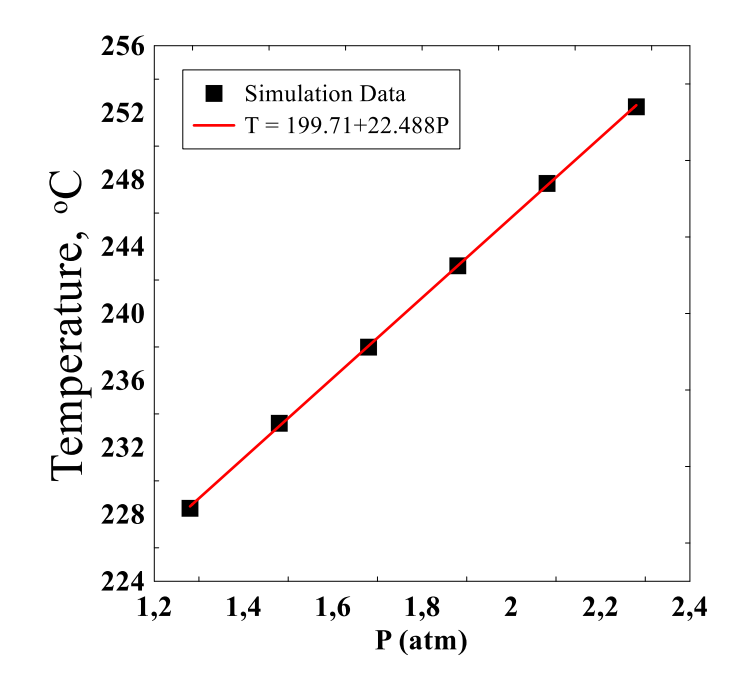


Figure S7. Pressure compensated control loop pressure vs. temperature setpoint relationship.

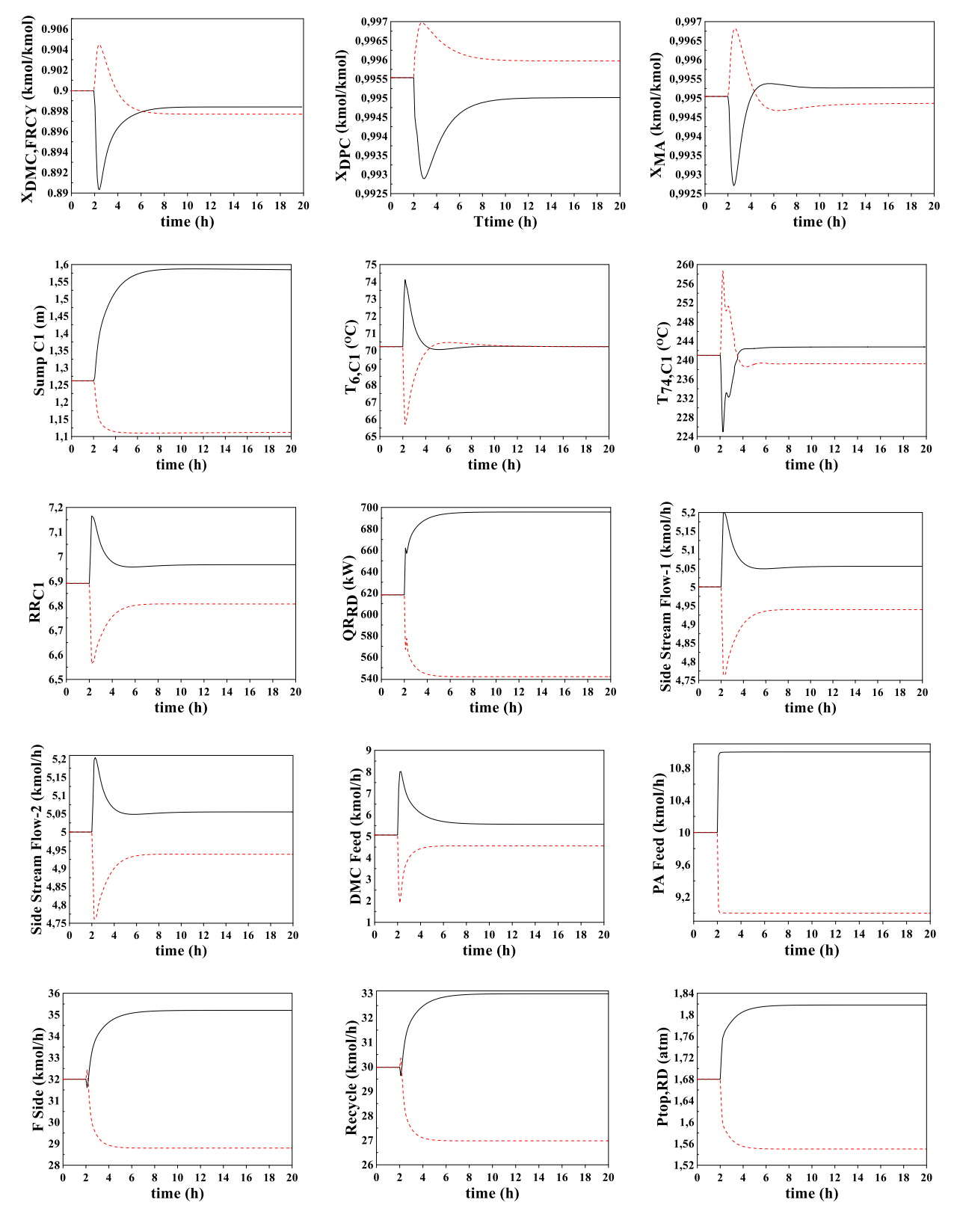
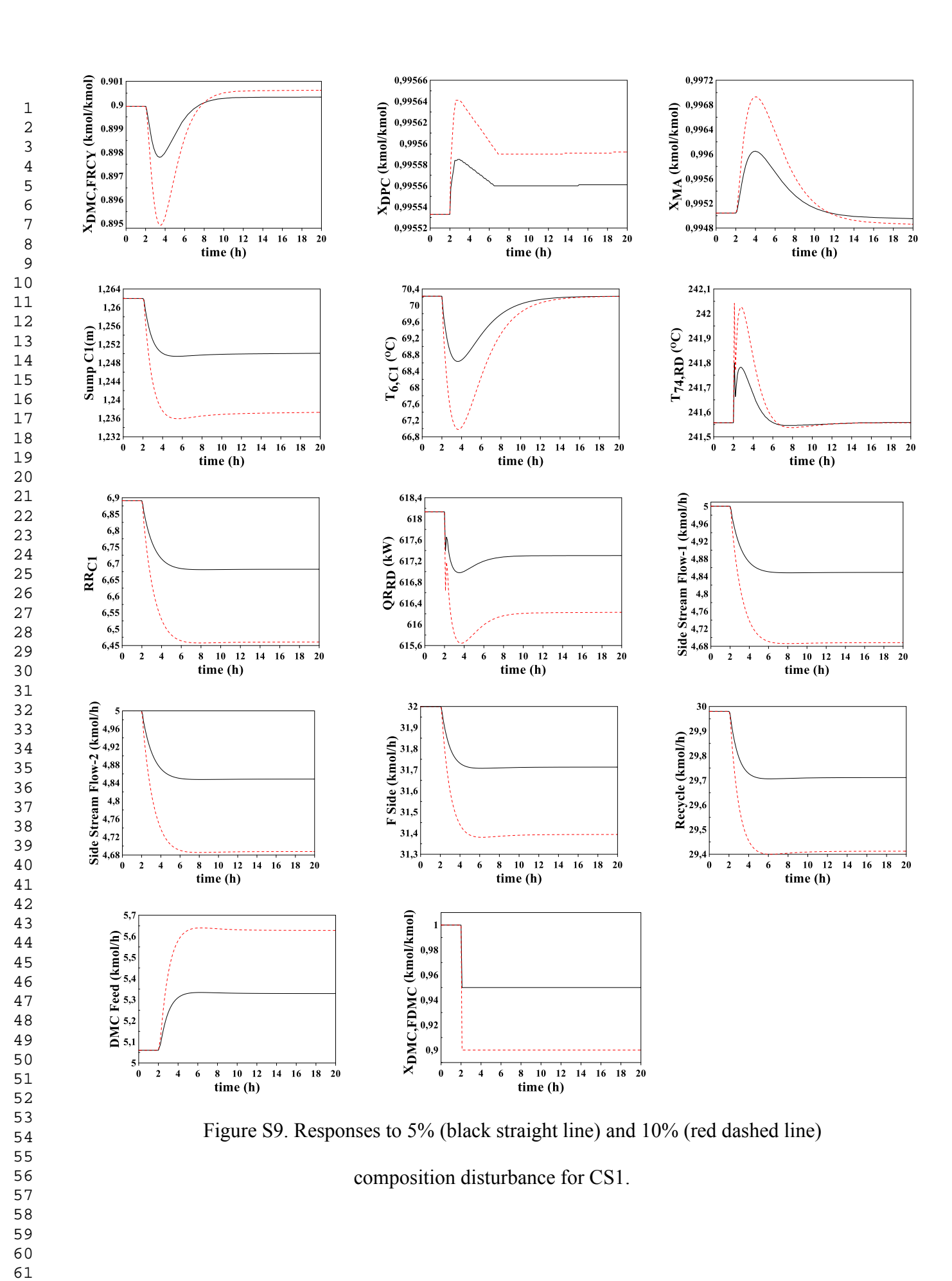


Figure S8. Responses to +10% (black straight line) and -10% (red dashed line) throughput disturbances for CS1.



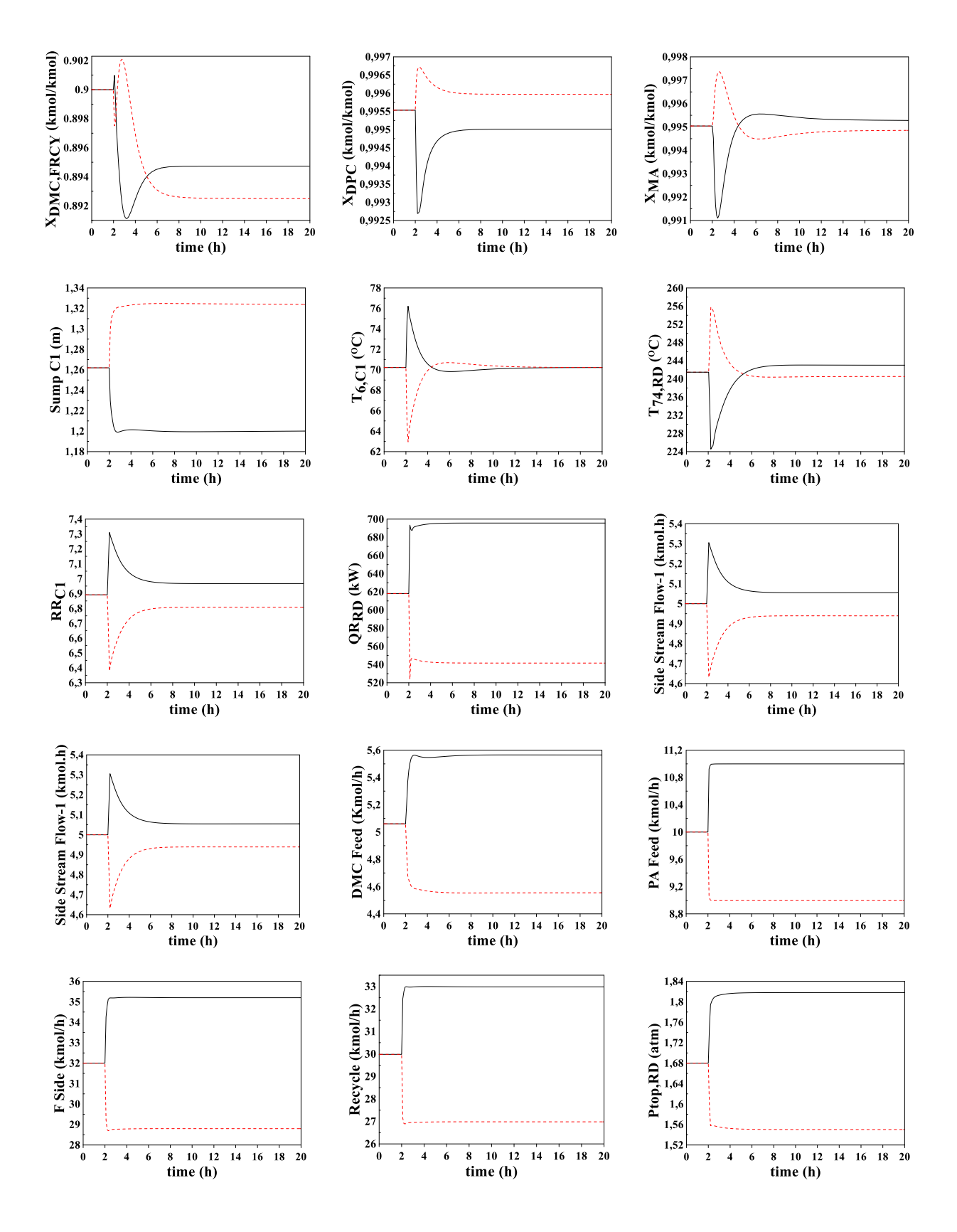
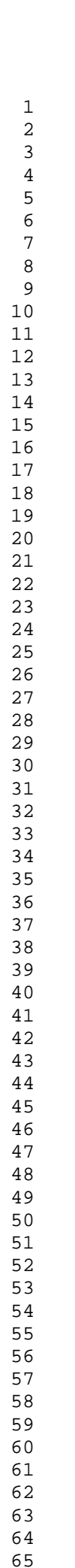


Figure S10. Responses to +10% (black straight line) and -10% (red dashed line) throughput disturbances for CS3.



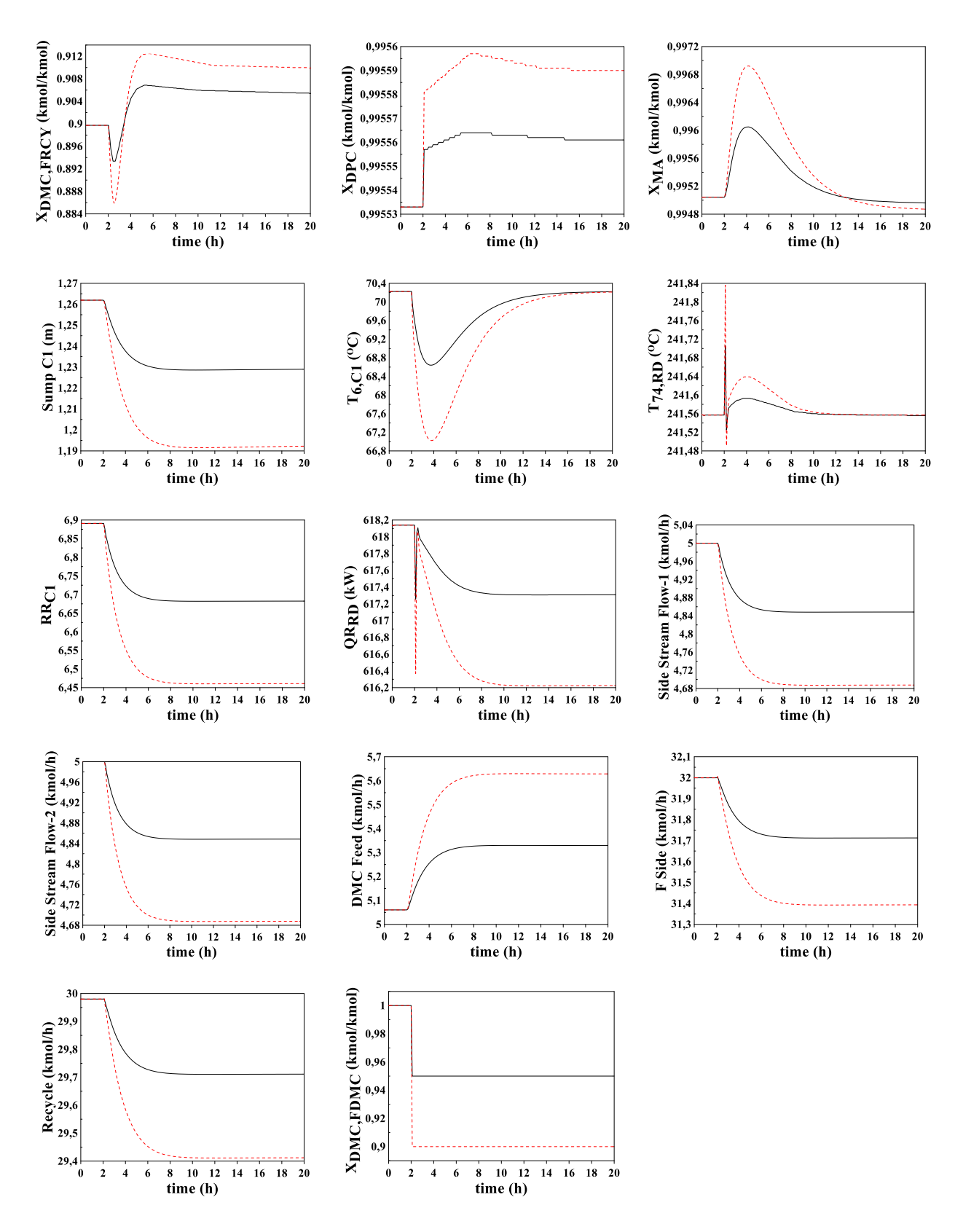


Figure S11. Responses to 5% (black straight line) and 10% (red dashed line) composition disturbance for CS3

Supplementary Data – Tables

Table S1. Kinetic parameters of the DPC synthesis

	$k_0 \text{ (m}^3\text{/kmol.s)}$	E_a (kJ/kmol)
k_{f_1}	135	54.200
k_{b_1}	52	54.900
k_{f_2}	1210	61.500
k_{b_2}	611	56.200
k_{f_3}	82.000	76.800
k_{b_3}	109.000	70.800

Table S2. Parameters of the Antoine Equation of each component in the DPC process

	MA	DMC	PA	MPC	DPC
C_{Ii}	49.74091	46.50691	79.76991	18.6074	82.8855
C_{2i}	-5618.6	-5991.3	-10074	-10121.3	-12708.4
C_{3i}	0	0	0	0	0
C_{4i}	0	0	0	0	0
C_{5i}	-5.6473	-5.0971	-9.4831	-7.82	-9.5761
C_{6i}	2.1E-17	1.34E-17	3.84E-18	2.54E-18	1.74E-18
C_{7i}	6	6	6	6	6

Table S3. Temperature Controller parameters for CS1 and CS2

Controlled	Manipulated	Controller	Kc	$ au_{ m I}$
Variables	Variables		(%/%)	(hr)
T _{74, RD}	Q _{C1}	TC1	1.27	1.29
T ₆ , C ₁	RR_{C2}	TC2	0.7	0.98

Table S4. Temperature Controller parameters for CS3 and CS4

Manipulated	Controller	Kc	$ au_{ m I}$
Variables		(%/%)	(hr)
Q _{C1}	TC1	1.77	0.87
RR_{C2}	TC2	1.1	0.66
	Variables QC1	Controller Variables QC1 TC1	Controller Variables (%/%) QC1 TC1 1.77

Declaration of Interest Statement

Declaration of interests

☑ The authors declare that they have no known competing financial interests or personal relationships that could have appeared to influence the work reported in this paper.	
□The authors declare the following financial interests/personal relationships which may be considered as potential competing interests:	
	_